Ontogenetic Influences on Endothermy in the Great White Shark (*Carcharodon carcharias*)

David C. Bernvi

Stockholms universitet

Abstract

The great white shark is endothermic. Ecophysiology in relation to endothermy is largely unknown yet may disclose life history ecology. An ontogenetic approach using the allometric equation estimates parameters related to endothermy via biometrics. Endothermy is hypothesised to constitute a temperature distribution mechanism and disclose ontogenetic life history ecology. Data was obtained from dissections. Results show that red muscle mass is isometric to body mass ($b = 0.97$, $n = 18$). Caudal fin height growth rate show negative allometry in juveniles but not for other size classes. Modulated burst swimming speed is highest for adults reaching maximum 58 km/h (mean sustained 9.3 km/h) and lowest for neonates reaching maximum 35 km/h (mean sustained 5.7 km/h). Sustained swimming speed is verified and used to estimate energy requirements *ex vivo*. Maximum stomach volume was isometric to body mass. A 23 kg neonate have a stomach volume of 1.7 l and requires 353 kcal/day, a 125 kg juvenile requires 1,206 kcal/day (stomach volume 12.1 l), a 350 kg sub-adult requires 2,382 kcal/day (stomach volume 39.8 l) and a 900 kg adult great white shark required 4,871 kcal/day (stomach volume 119.7 l). Maximum stomach volume is used to extrapolate on feeding requirements to determine optimal prey. Metabolic estimates are 22-64% underestimated compared to previous *in vivo* measurements. Results show that great white sharks have the same routine metabolic scaling rate as birds and bats ($b = 0.71$, $P = 0.3$). An ontogenetic heat production model presented for red muscle mass coincides closely with previously published field measurements of body temperature in the tissue adjacent to red muscles. Red muscle temperature independent of body size is $19.1\pm1.8°C/kg\ h^{-1}$ without heat loss. Results suggest that the great white shark transfer heat within the body as previously proposed for tunas. Heat production from red muscles and specific dynamic action increase the stomach temperature to a temperature of $25.9\pm1.1°C/kg\ h^{-1}$ independent of body size. The mass specific heat production for adults is approximately half of that found in neonates and scales ($b = -0.31$), closely to the inverse scaling of the surface rule. Heat production in stomach coincides with pervious *in vivo* measurements. Stomach heated digestion probably limit the distribution of this species in colder waters.

Keywords

Populärvetenskaplig sammanfattning

Vithajen är endotermisk men mycket om dess livshistoria kopplat till varmblodigheten är okänt. Genom att studera tillväxt kopplat till de värmealstrande röda musklerna kan delar av vithajens liv förklaras. Hypotetiskt bör varmblodigheten begränsa vithajens utbredning relaterat till vattentemperatur under tillväxten. Genom dissektioner samlas data som visar att massan röda muskler är proportionell till varmblodigheten. Tillväxten är dessutom högre för juveniler än hos andra livsstadier. Simhastigheten moduleras och visar att en vuxen vithaj kan nå högst 58 km/h. Även magvolymen mäts och kan uppnå över 100 liter. Med hjälp av simhastighet beräknas vithajens metabolism och optimala bytesdjur för olika storleksklasser kan klarläggas. Vithajens metabolism skalar på samma sätt som hos fåglar och fladdermöss men är olik däggdjur generellt. Modeller för värmeproduktionen presenteras. För att värma magsäcken respektive hjärna, ögon och muskler omkring de värmealstrande röda musklerna bör vithajen värmeväxla precis som tonfiskar. Detta är möjligt genom att förflytta värme via blodet och genom att konvektion värmer upp olika organ beroende på behov. Konduktionen är också viktig för att värma upp magsäcken och kringliggande muskler till de röda musklerna. På detta sätt kan vithajen få ut mer av sina värmealstrande röda muskler. En modell för magtemperaturen visar att magsäcken har en temperatur på 25.9±1.1°C oberoende av vithajens storlek och kan bekräftas av tidigare studier. Uppvärmningen av magsäcken är troligen en begränsande utbredningsfaktor.

Nyckelord

Above: The author (*David Bernvi*) dissecting a great white shark *Carcharodon carcharias* in the wet-laboratory at the KwaZulu-Natal Sharks Board in Durban, South Africa. Picture: Paul von Blerk.

Cover: An approximately 4 meter in total length great white shark breaching at a seal decoy in False Bay, South Africa. Picture: Gaspare Schillaci

Table of contents

1. INTRODUCTION

1.1 Evolved to produce heat

The great white shark *Carcharodon carcharias* is a highly active apex predator with the most wide-ranging distribution among fishes (Compagno 2001). As a pelagic ram-ventilating endothermic predator (Carey *et al.* 1985, Bonfil *et al.* 2005), utilising a thunniform swimming mode (Graham 1990), the great white shark is capable of bursts of speed of 35-43 km/h (Martin & Hammerschlag 2012). The thunniform swimming mode is the most efficient aquatic locomotion mode evolved in vertebrates, allowing thrust generated by a lunate shaped caudal fin to generate lift while lateral movement only occurs in the posterior part of the body with no undulation in the anterior body which reduces friction (Sfakiotakis *et al.* 1999). Explosive predatory breaching events where the great white shark reaches over 2.4 meter above the water surface, targeting e.g. Cape fur seals *Arctocephalus pusillus,* are commonly observed and well documented in South Africa (Martin & Hammerschlag 2012, Fallows *et al.* 2012, Martin *et al.* 2005). This ability of the great white shark is likely to be correlated to the endothermic capacity. The great white shark is born at 12 kg body mass and may reach 2,000 kg body mass as an adult (Compagno 2001); this 167 factorial increase in body mass is hypothesised to be proportional to endothermic capacity due to the surface rule. The surface rule indicates small animals have a ratio of larger surface area to body volume while large animals have a smaller surface area to body volume (Schmidt-Nielson 1984). This means small animals have higher heat loss due to the larger ratio heat emitting surface area to heat conserving body volume.

In this study the endothermy of the great white sharks is investigated from specimens collected at the KwaZulu-Natal Sharks Board (KZNSB) in South Africa. Endothermy is elucidated in light of ontogenetic development to explain temperature distribution and life history. The endothermic capacity is hypothesised to play a central role in the development of the great white shark's ability to predate and inhabit the colder habitats e.g. upwelling areas where high energy prey, e.g. marine mammals, occur. Endothermy may also play an important role in trans-oceanic migrations to important foraging areas and while conducting drift diving behaviour enabling movement into deep and colder waters (Bernal *et al.* 2012, Bonfil *et al.* 2005, Boustany *et al.* 2002).

The morphology of family Lamnidae present adaptaptions only found in the fastest fishes of the ocean (Carey 1982, Carey *et al.* 1971, Compagno 2001). The spindle shaped body, a large and highly symmetrical caudal fin, conical snout and regional endothermy in red muscles, eyes, brain, stomach and viscera (McCosker 1987, Block & Carey 1985, Alexander 1998) added to the formidable body size in the great white shark, bears witness to a powerful predator in its own league. Regional body temperatures in the viscera and stomach may reach up to 14°C above the ambient environment (Goldman *et al.* 1996, Lowe & Goldman 2001), which indicate a highly active digestive system, as found in tunas (Fritzgibbon *et al.* 2006). The large gills are indicative of high oxygen consumption, which reflect a high metabolic rate, essential to retain regional body heat (Ezcurra *et al.* 2012, Bernal *et al.* 2005, Graham *et al.* 1983). Red muscles are positioned close to the vertebral column, rather than subcutaneously on the lateral side as in ectotherms, to reduce conductive heat loss (Carey 1982, Carey *et al.* 1985). Red muscles are used during sustained swimming and their internal position makes it possible to retain produced heat (Carey *et al.* 1981, Carey *et al.* 1982, Carey *et al.* 1985, Bernal *et al.* 2005). The heat retention by convective heat

transfer is significant due to the counter-current capillary network known as *retia mirabilia* extending between the red muscles and subcutaneous lateral vessels (Carey & Teal 1969, Carey *et al.* 1985, Bernal *et al.* 2005, Bernal *et al.* 2012). Moreover, red muscles are highly vasculated and contain high amounts of myoglobin making red muscles suitable for continuous but slow swimming (Sepulveda *et al.* 2015, Carey 1982). The paler surrounding muscles are fast twitching and less vascularised but are important during burst swimming (Syme & Shadwick 2011, Carey 1982); they also function as an isolating temperature gradient to the red muscles (Bernal *et al.* 2012). The counter-current capillary network creates a temperature gradient between cold oxygenated blood reaching the red muscles from the gills and warm deoxygenated blood flowing to the heart (Carey *et al.* 1971). This increases the metabolic efficiency of the red muscle (Carey 1982) which may reach temperatures 3-5°C above the ambient water for a 4.6 meter great white shark (Carey *et al.* 1982) and 3-4°C above the ambient water temperature for a 3.5 meter great white shark (Tricas & McCosker 1984).

There are also other endothermic specialisations in other parts of the body to reduce heat loss via convection of the blood with counter-current systems, such as the suprahepatic organ in front of the liver, positioned around the oesophagus to increase the temperature in the viscera (Carey *et al.* 1981). The temperature in the stomach of the great white shark has been reported to have a consistent mean of 26°C from five field studies (Goldman 1997, Goldman *et al.* 1996, Lowe & Goldman 2001, McCosker 1987). Warm blood from red musculature also heats important organs like brain and eyes via drainage into cerebral sinuses through the anterior red muscles via two red muscle veins (Wolf *et al.* 1988). Coiled pseudobranchial vessels bring cold oxygenated blood from the gills ventrally to the neurocranium that is heated before reaching the brain and eyes (Block & Carey 1985, Alexander 1998). The vascular system of the great white shark and other close relatives (Lamnidae) also show intriguing specialisations e.g. the dorsal aorta is rudimentary (Burne 1923) and thus most of the blood from the trunk is rather derived via the lateral subcutaneous vessels instead of above the body cavity via dorsal aorta (Carey *et al.* 1985, Bernal *et al.* 2012).

The great white shark's endothermic adaptions are positioned between the mako shark in the genus *Isurus* and the porbeagle shark in the genus *Lamna* (Carey *et al.* 1985). The great white shark has less developed morphological cold water adaptations than the porbeagle *Lamna nasus* and salmon shark *Lamna ditropis* in terms of red muscle mass and the number of vessels in *retia mirabilia* however is, better adapted to cold water than the two species of mako shark in the genus *Isurus* (Carey *et al.* 1985). It is notable that the evolutionary relationship among lamnids (Compagno 1990) also reflects their endothermic capacity. Endothermy may thus be an ancient adaptation evolved in the family Lamnidae.

1.2 Ontogenetic allometry

To study the temperature tolerance in the great white shark during its life history, the ontogeny of endothermy needs to be understood. The development of anatomical traits in the same individual during the life span, having different growth rates during different life-stages, are known as ontogenetic allometry (Cheverud 1982). Ontogenetic allometry describes traits as they change relative to body size during ontogenesis (Pélabon *et al.* 2013). If however the growth rate is directly proportional to the relative body size the growth rate is isometric and not allometric (Huxley & Tessier 1936) i.e. the organ is growing larger with no proportional difference to the rest of the measured body size.

To describe ontogeny, the morphometrics of different individuals is measured and described using the allometric equation (Huxley 1924, von Bertanlanffy 1960, Gould 1966). Linear regression analysis is used on log transformed allometric functions (Schmidt-Nielsen 1997, Huxley 1924).

The growth pattern may be isometric or allometric (Huxley & Tessier 1936). If the growth is isometric the growth rate is the same for the two variables investigated (slope = 1). If there is a slower growth for the dependant variable, the growth rate for that variable is said to show negative allometry (slope <1) and if the growth rate is faster for the dependent variable (slope >1) the growth rate is said to show positive allometry (Huxley & Tessier 1936).

Allometry for the great white shark and other sharks has been studied using linear regression analysis, mostly for body length to body mass relationships (Bass 1973, Bass *et al.* 1975, Casey & Pratt 1985, Cliff *et al.* 1989, Mollet & Cailliet 1996). However, few studies investigate specific organs and their proportions relative to ontogenetic growth to understand the ecological implications during life history. The allometric relationship of the great white shark's dentition has been sought because of is important forensic role in investigating shark attacks (Nambiar *et al.* 1991) and the caudal fin allometry and liver allometry was investigated in Lingham-Soliar (2005a).

It is well known that the great white shark adapts to a broader diet including marine mammals as it attains 3-3.5 meters total length (Tricas & McCosker 1984, Hussey *et al.* 2012, Hubbell 1996, Carlise *et al.* 2007). The ontogenetic dietary shift may also be related to an endothermic shift.

1.3 Rationale

To investigate the role of endothermic capacity during ontogeny, the great white shark is classified into four different size classes according to Hussey *et al.* (2012), namely; neonates, juveniles, sub-adults and adults (Table 1). By using those delimiting life-history stages the ontogenetic morphological and physiological traits may be statically tested in allometric functions and their scaling parameters elucidated.

The overall aim of the present study was to investigate if the physiological traits involved in thermoregulation, including swimming capacity, energy requirements and heat production, influence ontogentic changes in great white sharks.

To elucidate this, the red muscle mass was estimated and related to body mass in order to test if the red muscle proportion is larger in adults. Few great white sharks have previously been measured for red muscle proportions. In Carey *et al.* (1985) red muscle mass is reported to increase by 66% in a single adult compared to the mean of neonates, juveniles and sub-adults. By increasing the number of samples from great white sharks, especially from neonates, juveniles and sub-adults, results should hypothetically show a gradual increase in red muscles mass as the shark grows and adapts to colder water, as hypothesized by Carey *et al.* (1985).

By modulating swimming speed using Sambilay (1990) and the caudal fin biometrics it is possible to estimate the heat production of red muscles in the trunk as well as for the total body mass. The routine metabolic rate and daily energy requirement was also estimated based on the kinetic energy used from the modulated swimming speed. Stomach volume was measured to extrapolate optimal prey based on different energy content. The caudal fin height and caudal fin area was measured for different size classes and used to calculate swimming speed and to determine possible habitat preference and growth rate during life history using the caudal fin aspect ratio.

The development of endothermy may be related to one or several ontogenetic dietary shifts in the great white shark. The known dietary shift result in predation towards high calorie prey in temperate areas targeting marine mammals, shifting from predation on mainly teleosts and elasmobranchs in sub-tropical areas (Klimley 1985, Hussey *et al.* 2012). During ontogenetic development the great white shark loses the narrow shaped teeth and wider more triangular teeth develop which enable increased predation on marine mammals, reaching proportions of 47.6% of the total adult diet (Hussey *et al.* 2012, Hubbell 1996, Tricas & McCosker 1984). Great white shark abundance has been observed to rapidly decrease in waters below 11-13°C (Compagno 2001, Ferreira & Ferreira 1996) suggesting a preference for higher temperatures. The shift to predation on marine mammals in cold temperate waters (Klimley *et al.* 1996) suggests there may be a trade-off between increased availability of high calorie prey species and the greater energy requirements associated with colder waters.

Hypotheses of the study
1. Is there a gradual increase in the proportion of red muscle mass as the great white shark grows and adapts to wider distribution-range i.e. colder waters?
2. Can the temperature threshold for lower temperatures in the great white shark be defined by using red muscle mass and body size (length/body mass)?
3. Are there any gradual ontogenetic differences in endothermic capacity in great white sharks? If there is a difference between adults and juveniles in terms of temperature preference, can this then be interpreted as part of the dietary shift towards marine mammals evident in adult great white shark morphology, e.g. in widening of teeth?

2. MATERIAL & METHODS

2.1 Study area and collected specimens

All great white sharks examined in this study were incidentally collected through the KwaZulu-Natal Sharks Board shark control-program using beach protective nets and experimental drumlines (Cliff *et al.* 1988, Cliff *et al.* 1996, Cliff & Dudley 2011) along the popular beaches in the South African KwaZulu-Natal province. The beach protection nets are positioned at 38 locations (Cliff & Dudley 2011). The number of individual beach protective nets varies depending on location. The beach protective net consists of a yellow polyethylene braid gill net being 214-304 m long and 6.3-7.3 meter deep anchored 300-500 meters from the shore and paralleled to the beach in water depth ranging from 10-14 meters. The nets have a stretched mesh of 51 cm with a braking strain of 160 kg and are secured with a 35 kg anchor at each end. The beach protective nets are inspected early in the morning each working day, if weather conditions so permit, with a total of 15-20 inspections monthly (Cliff *et al.* 1988, Cliff & Dudley 2011).

Experimental drumlines have been introduced at 19 of the 38 locations and serve to reduce by-catch while targeting large potentially dangerous sharks such as great white sharks, tiger sharks *Galeocerdo cuvier* and bull sharks *Carcharhinus leucas*. An experimental drumline consists of a baited hook (Mustard hook 4480DT 14/0 J Gjøvik, Norway) connected to a chain and hanging from a large floating device anchored adjacent to a protective beach net. The survival rate of drumline-caught animals is similar to that for beach protective nets (Cliff & Dudley 2011). Live animals are

released and tagged from the beach protective nets and experimental drumlines on inspection (Cliff & Dudley 2011) while dead animals are returned to shore for scientific research, where they are weighed, measured and dissected. During the sardine run season both the beach protective nets and drumlines are temporarily removed to prevent excessive catches.

In total, allometric data from 314 great white sharks collected by the KZNSB was used for this study. Of these 18 great white sharks were used to estimate the red muscle distribution (6 dissected by the author) and 5 great white sharks that were used for stomach volume estimation by the author of the present report. Additionally, data collected by Dr. Enrico Gennari from 12 great white sharks collected at the KZNSB between 2009-2011 were also used for red muscle distribution analysis.
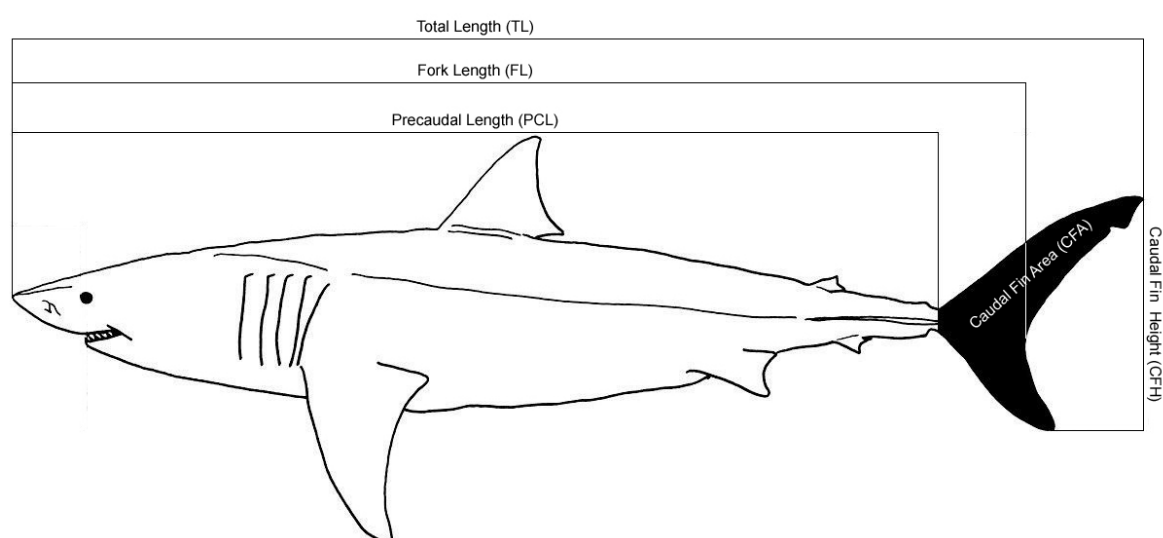
2.2 Measurements

Figure 1: Measurements used; total length (TL) the body length from snout tip to dorsal caudal fin tip in natural position, fork length (FL) from snout tip to middle caudal fin notch, precuadal length (PCL) from snout tip to precaudal pit, caudal fin area (CFA) the area (black area in figure) of one side of the caudal fin and caudal fin height (CFH) the distance from dorsal tip to ventral tip of the caudal fin.

Standard measurements (Compango 2001) were collected (fig.1) by KZNSB and the author and include total length (TL) with caudal fin in natural position. Fork length (FL) was used to determine position and length of cross sections (Carey *et al.* 1985). The precaudal length also called standard length (PCL) is least prone to measuring errors compared to TL and FL since the plasticity of the caudal fin is excluded (Cliff *et al.* 1996), hence PCL is primarily used in calculations. A new measurement, caudal fin area (CFA) was also measured, defined as one side of caudal fin surface area (Sambilay 1990). Also the caudal fin height (CFH), the distance between the caudal lobes, tip to tip was measured. The CFA, CFH and PCL may be used to estimate the swimming speed (Sambilay 1990) in a great variety of fish species. CFA was also used to study the allometry of the caudal fin. Body weight is called body mass (BM). All measurements taken were measured in millimetres (mm) and for mass in kilograms (kg).

Body length measurements were taken off the great white shark by placing a metric tape on the floor and the shark's pectoral or dorsal fins on top not disrupting the measurement. To make sure

the measurement started at the snout tip a specially designed freestanding board was used inserted beneath the great white sharks head (fig 2). Body mass was measured using an analogue scale and hoist capable of weighing up to 1,000 kg.

Figure 2: Measuring technique demonstrated on a juvenile female great white shark (UMH15006). To make accurate large body measurements in millimetres a specially developed freestanding board was used inserted under the head. The metric tape was placed in a straight line off the body and beneath fins not to be disrupted by body shape.

2.3 Dissection protocol

Gutting

Gutting was done before cross sectioning as soon as the specimen had defrosted for 24-36 hours. A ventral sagittal incision was made carefully from the opening of the vent ventrally along a midline of the stomach with a knife. A finger was inserted into the body cavity while the knife was angled 30° to avoid cutting through the liver or stomach. The incision ended at the start of the pericardial diaphragm. After the organs of the body cavity had been removed also the pericardium was opened cutting through the pectoral girdle cartilage. The body wall was also cut dorsoventrally trough the marked cross section lines (fig. 3).

Each liver lobe was cut free from the suprahepatic rete including the gall bladder with a scalpel. The stomach was cut free from the suprahepatic rete at the end of the oesophagus. If the stomach were accidentally ruptured the opening was stitched together using a nylon tread (Ø1 mm). The viscera were removed caudally at the vent opening with scissors. The epigonal organ and gonads were removed with a scalpel from the suprahepatic organ and the dorsal body cavity with scissors. The heart was removed from the pericardium with scissors. The suprahepatic rete was removed with a scalpel and separated from the oesophagus before weighing.

Cross-sectioning

Great white sharks were cross-sectioned in 12 places between the 4th gill slit and the precaudal pit, following the procedure of Carey *et al.* (1985). Cross sections were cut into 5% pieces of FL (Carey *et al.* 1985). The first incision were cut at 27% of FL and continuing with 5% of FL for each section until the 12th section have been defined at 87% of FL ending at 92% of FL, a modification from

Carey *et al.* (1985) adding additionally 2% FL posteriorly for the incisions. In total 60% of the FL were cut in to 12 cross sections.
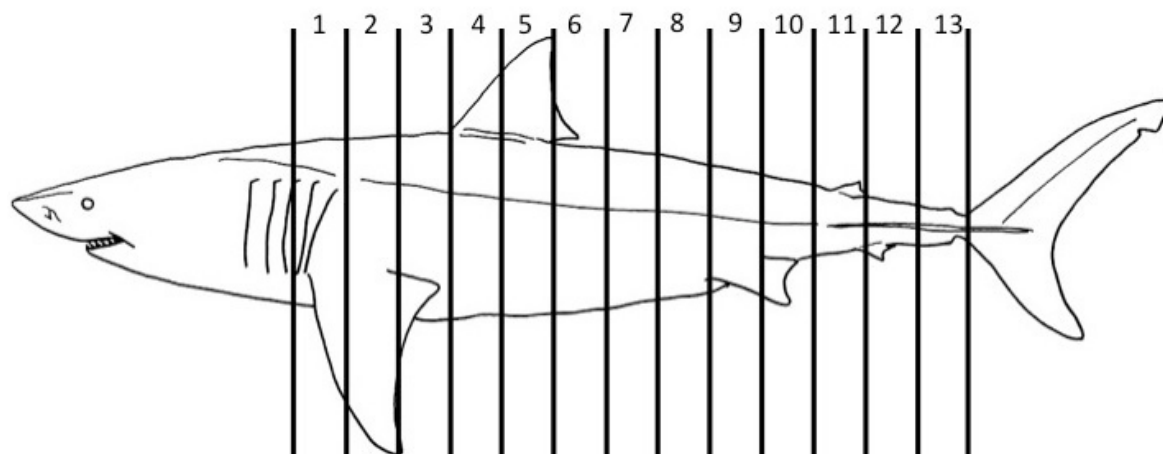

Figure 3: The position of the cross sections made in this study of the great white shark. The most anterior cross sections start at 27% of FL and the most posterior cross section ends at 92% of FL. Each cross section length was 5% of FL. More cross sections increased the accuracy of the red muscle area distribution analysed as a mean of 12 cross sections. However results show 13 cross sections were possible to dissect for some great white sharks but the last 13th cross section lacked red muscles.

The cross sections were marked before cutting using a ruler and chalk/pencil to indicate the positions of incisions and marked with a number before the first cut, while a metric tape placed off the specimen was used to determine the cross section length. Rechecking was done for the positions of incisions before any cutting began. A photograph of the great white shark's length covering the full PCL-measurement was taken with the marked sections before the cutting began to ease comparison with historical data and similar specimens in the future.

To ensure the marks printed by chalk or pencil did not wash away, a small epidermal incision for each cross section mark was done with a scalpel. The first dorsal and pectoral fins were also cut away to ease the cross sectioning. The incisions were made with ±1 cm certainty and were hand cut with a big knife. Cuts were made as clean possible.

2.4 Photographing

External body
All photographs were taken with a system camera (CANON EOS 700D) in highest resolution possible and a metric ruler was adjacent to the specific specimen. Photographs were mainly taken in daylight outdoors or on the dissection table.

Cross sections
The cross sections were placed horizontally flat with the posterior side up, instead of the anterior side up as described by Carey *et al.* (1985), adjacent to a graduated ruler in the camera frame. The rearrangement from anterior position to posterior position of the cross section photograph was done due to the remarks of the red muscle distribution placed more posterior in great white sharks compared to other lamnids (Carey *et al.* 1985). The camera was close to a 90-degree angel

approximate 1 meter above the specimen covering the total cross section area in the camera frame (fig. 4). The background of the photograph was mono-colour bright. The photos were taken outside or in a well-lit area with particular care taken to the contrast in the photograph to visualize the difference between red and white muscles. Cross sections were washed clean individually from blood and tissue pieces before photographing and special care was taken around the margin of the red muscle area to make it clear and clean cut. If the cut was not cut clean, surface cuts were made with scalpel and scissor to arrange the incision correctly.

2.5 Estimation of area, volume and mass

Area estimation

The red muscle area distribution in cross-sections was estimated using the computer software NIH (National Institute of Health, USA) ImageJ version 1.47. The ruler in each cross section photograph was referred to as a scale. The image was converted into composite grey

Figure 4: Photographs were taken on the cross section posterior part approximately 1 m above the specimen in 90° angle to the camera. A metric ruler was placed next to the specimen as a scale.

scale to easier determine the red muscles. After this the image was processed in binary black and white condition making it possible to auto select the red muscle area for measurement without observer bias. In some photographs this was not possible due to the diffuse contrast or unclear cuts and the selection had to be made by hand on a composite grey scale image. Observer bias of hand selected area was however insignificant and usually lower than software auto selection. Diffuse contrast may be a source of error not mentioned in Carey *et al.* (1985). Only the side of the cross section lacking *livor mortis*, i.e. the side of the shark that had not been placed against the ground shortly after death was used to estimate the red muscle area. The corrupt lateral side is easily detectable by the disfiguration in body shape i.e. flattening of the lateral side in the cross section. Lateral side with *livor mortis* varied. This potential source of error has been disregarded in previous studies (Carey *et al.* 1985, Bernal *et al.* 2003). The red muscle areas from cross sections were used to establish the mean red muscle area (MRMA) by measuring one side and then multiplying with 2 for each cross section to make the total area in a cross section. MRMA was determined by an arithmetic mean.

The area of the caudal fin was also estimated using the same software and a scale was fitted to the image from a ruler. Selection was done by hand or using the auto selection tool.

In view of the paucity of values, caudal fin surface area, a relationship using the allometric equation was used from the specimens where this data was collected to estimate this variable for the great white sharks where no caudal fin surface area measurements exists.

Volume estimation

The volume of the red muscle (V_{RM}) was estimated in cm^3 with the cylinder shape. The mean red muscle area created the area in cm^2 and 60% of the FL (used to make cross sections) in cm created the height of the cylinder.

$$V_{RM} = MRMA \cdot 0.6FL$$

The volume of the stomach was estimated by filling the stomach with water using a hose while the stomach was contained in a plastic bag. The plastic bag and stomach was lifted up in a hanging position so that the stomach could be filled with water to it's maximum without a deformation from a flat surface. If there was a leak in the stomach wall a nylon tread (Ø1 mm) was used to stitch it together. The water from the full stomach was then contained in a vessel to be measured in a 1000 ml cylinder. This procedure was done twice and the maximum value used as measurement. The stomach was greatly expandable.

Mass estimation

The only mass estimation done was that for red muscles. It was merely impossible to dissect out the red muscles and measure the mass. The trunk red muscle mass (TRMM) in kg was estimated adapting the tissue density (*d*) from (Alexander 1959; Bernal *et al.* 2003) of 1.05 g/cm^3 and V_{RM} from this study in cm^3. The tissue density is the same for mako shark *Isurus oxyrinchus* and cyperids and may be used for most fish species.

$$TRMM = \frac{V_{RM}d}{1000}$$

2.6 Data analysis and the allometric equation

Red muscles analysis

Mean red muscle area was calculated from the 12 cross sections for each individual (*n* = 6) and an additional sample of (*n* = 12) great white sharks with 4-6 cross sections, photographed by Dr. Enrico Gennari. Both anterior and posterior views of those 12 specimens were photographed which made it possible to determine 8-11 cross sections in posterior view. Anterior positions mirror posterior cross section in the cross section positioned prior to the photographed cross section. The positions of those cuts where checked against the position from the 6 specimens dissected by the author. If it was not possible to correlate the position of the cuts between specimens from the author and Dr. Enrico Gennari, the additional cross section photographs for those cross section were not used hence the difference in the number cross section photographs used from Dr. Enrico Gennari. The resolution of the red muscle distribution was lower with fewer cross sections; nevertheless the distribution of red muscles in sharks with fewer cross sections was useful to estimate the mean red muscle area for the entire sample, in total 18 great white sharks.

The allometric equation (eq. 2.6a) was used to study the ontogenetic growth. A null hypothesis was set to isometric growth i.e. no differential growth of red muscles as observed in elasmobranch muscles (Bernal *et al.* 2003). The slope (*b*) and scaling coefficient (*a*) of the allometric equation, is

expressed as the function of (M_{BM}), raised to the power of (b) and multiplied by the scaling coefficient (a), the independent variable is thus on the x-axis (M_{BM}). Intersect of the function is the scaling coefficient (a). The resulting dependant variable (TRMM) of the function is (y). Body mass (M_{BM}), is not always adopted but commonly used. Isometric growth reflects geometric similarity between the independent and dependent variables tested.

Equation (2.6a)

$$y = aM_{BM}^{b}$$

The scaling exponent b was tested against the null-hypothesis stating isometric growth, in this case mass-on-mass isometry is ($b = 1$). For growth ($b > 1$), positive allometry exists and for growth ($0 < b < 1$), negative allometry exists, if ($b = 0$) independence exists and if ($b < 0$) inverse allometry exists (i.e. the dependent variable is decreasing instead of growing). Isometry is different depending on what dimensions that are tested. If tested against length-on-length, or any other variables of the same dimensions, slope for isometry is 1 ($b = 1$), but for length-on-mass isometry the slope is $\frac{1}{3}$ ($b = 0.333$) and reverse $\frac{3}{1}$ ($b = 3$). Testing metabolic rate to mass for mammals isometry is $\frac{3}{4}$ ($b = 0.75$) i.e. mammalian resting endothermy (Schmidt-Nielsen 1984) and if the metabolic rate is totally surface dependant according to the surface rule, the slope for isometry is $\frac{2}{3}$ ($b = 0.67$) i.e. ectothermy Schmidt-Nielsen 1984). Testing for area to length isometry is $\frac{2}{1}$ ($b = 2$). Hence, this emphasizes the importance of knowing the expected isometry for independent and dependant variables tested.

The ratio between trunk red muscle mass (TRMM) from the cross sections per specimen and body mass (BM) was used to estimate the proportion (%) red muscles (RM%) of body mass (Eq. 2.6b).

Equation (2.6b)

$$RM_{\%} = \frac{TRMM}{BM} \cdot 100$$

To test the red muscle growth for allometric relationship to trunk red muscle mass and body mass were used in the allometric equation where body mass was the independent variable and trunk red muscle mass the dependant variable.

Allometry for caudal fin

To estimate the relationship between body length, precaudal length, PCL (m) and caudal fin height, CFH (m) was used and tested for isometry ($b = 1$). The specimens were classified according to Hussey *et al.* (2012) in four different PCL delimiting classes. Neonates < PCL 1.85 m, juveniles PCL 1.85-2.349 m, sub-adults PCL 2.35-2.849 m and adults PCL $\geq$ 2.85 m. Table 1 show the PCL corresponding to total length (TL) and body mass (BM). All size classes were also tested together to give an allometric relationship for the species, since this is interesting when comparing evolutionary interspecies relationships *sensu* Lingham-Soliar (2005a). By testing each size-class separate it was possible to check that the data is not skewed due to larger sample size in one of the size-classes.

Table 1: Size classification (size-classes) based on life history stage by precaudal length (PCL) (Hussey *et al.* 2012), showing corresponding body mass (BM) and total length (TL) estimate intervals for South African great white sharks (Cliff *et al.* 1996).

Measurement	Life History Stage			
	Neonate	Juvenile	Sub-adult	Adult
PCL (m)	<1.85	1.85-2.349	2.35-2.849	$\geq$ 2.85
TL (m)	<2.381	2.381-3.012	3.012-3.645	$\geq$ 3.646
BM (kg)	<101	101-204	204-360	$\geq$360

Maximum stomach size

The stomach volume measured from 5 specimens was measured and investigated for isometry as the null hypothesis (b =1). The independent variable was BM (kg). The stomach volume in millilitres (ml) was the dependent variable. Mass and volume is of the same dimension as mass is the same as volume but where the density is known. Both quantities have three dimensions.

Swimming speed to estimate heat production and oxygen consumption

To estimate the heat production in trunk red muscle mass and body mass, the swimming speed model (eq. 2.6d) based on caudal fin aspect ratio (CFAR) and precaudal length in cm (PCL) was adopted (Sambilay 1990). PCL is also the standard length. To calculate the aspect ratio (CFAR) in equation (2.6c) of the caudal fin, caudal fin height (CFH) and caudal fin area (CFA) were used.

Equation (2.6c)

$$Caudal\ fin\ aspect\ ratio\ (CFAR) = \frac{(CFH)^2}{CFA}$$

Measurements for CFH (mm) and PCL (mm) were collected (n = 314) by KZNSB from 1994-2015 and CFA (mm^2) was measured from photographs (n = 8) in this study in order to extract the allometric relationship between CFA and CFH. The allometric relationship between CFA and CFH was then used to estimate CFA for specimens were the surface area had not been photographed, as described above for caudal fin area estimation.

Burst swimming speed and sustained swimming speed was estimated (eq. 2.6d) by using the equation in Sambilay (1990) where absolute speed in kilometres per hour (km/h) was possible to modulate and where M is the mode of swimming speed (0 = sustained swimming and 1 = burst swimming).

Equation (2.6d)

$$\log(km/h) = -0.828 + 0.6196 \log(PCL) + 0.3478 \log(CFAR) + 0.7621(M)$$

The sustained swimming speed may be used to estimate the heat production generated per second in the body mass for a great white shark with a certain precaudal length (PCL) and caudal fin aspect ratio (CFAR). Water temperature and body depth ratio (i.e. length/body depth) have no significant correlation to swimming speed (Sambilay 1990). The continuous velocity may be given from equation (eq. 2.6d) and defined as instantaneous acceleration i.e. constant velocity (eq. 2.6e). The instantaneous acceleration (a_{inst}) at time (t) is used to modulate the kinetic energy (E_k) in joule (J) from the sustained swimming velocity (eq. 2.6e). Using the body mass (M_{BM}) and constant velocity

(v) in meter per second converted from sustained swimming speed in km/h, the kinetic energy (E_k) expressed in joule (J) or in base units ($m^2 \cdot kg\,s^{-2}$) is given (Schmidt-Nielsen 1997).

Equation (2.6e)

$$E_k = \frac{1}{2} M_{BM} v^2$$

and

$$v = at$$

$$a_{inst} = \lim_{t \to 0} \frac{dv}{dt}$$

thus;

$$E_k = \frac{M_{BM} a^2}{2} t^2$$

and

$$\sqrt{E_k} = \frac{M_{BM} a_{inst}}{2} t$$

Because E_k is related to the acceleration (a^2) and time (t^2) square meter-mass per square second ($m^2 \cdot kg\,s^{-2}$) and not to instantaneous acceleration (a_{inst}) or time (t), the square root of E_k need to be formulated and expressed $\sqrt{E_k} = \sqrt{J}$ in base units ($m \cdot kg\,s^{-1}$), which educes the energy used for sustained swimming to a constant velocity from a non-increasing acceleration (a_{inst}) at any preferred time frame (t). The reason we are not using power, work per time unit, watt (W), also in J/s is because the base unit for Watt ($m^2 \cdot kg\,s^{-3}$) is adding one more power to velocity squared i.e. resulting in the power to three velocity (v^3). By using $\sqrt{E_k} = \sqrt{J}$ ($m \cdot kg\,s^{-1}$) and multiply with the time (t) in seconds (s) during sustained swimming we return to the Joule again ($m^2 \cdot kg\,s^{-2}$) i.e. $\sqrt{J} \cdot t = E_k$. This is because instantaneous acceleration is not time less but close to zero. The main difference is that we are not squaring the instantaneous acceleration and time but multiplying them to delimit E_k for a constant velocity at any given specific time frame.

An increase or change in velocity (v^2), i.e. acceleration or deceleration is of no interest but a constant velocity (v) over time frames such as hours or days (t) is of interest (eq. 2.6e). It may be easier to recognize that the time cannot be squared. Instead instantaneous acceleration is multiplied by time units i.e. a constant velocity multiplied by seconds to determine the kinetic energy during a chosen time frame.

The $\sqrt{E_k} \cdot t$ is only 25% of the total chemical energy used for muscles; the remaining energy product by the muscles is thermal energy i.e. 75% of the chemical energy (Schmidt-Nielson 1972). This proportion of kinetic energy is used rather than the 20% known from studies on ectothermic fishes (Bernal *et al.* 2003, Webb 1975) due to the fact that the great white shark is an endothermic fish and have mammal-like red muscles (Webb 1975). Hence heat production is three times higher than the kinetic energy used during sustained swimming speed and the total energy produced is four times higher than $\sqrt{E_k} t$.

Sustained swimming speed may be assumed to correlate with a majority of the routine metabolic rate (Ezcurra *et al.* 2012, Carlson *et al.* 2004, Graham *et al.* 1990, Sambilay 1990), because the great white shark is an obligate ram ventilator and continuously need to swim to oxygenate the body. Routine metabolic rate (RMR) is defined as volitional swimming after the nutrition in the

alimentary canal has been absorbed (Carlson *et al.* 2004). Specific dynamic action (SDA), the energetic cost of digestion and assimilation; usually is 15-20% in fish but higher in tuna reaching 35% (Carlson *et al.* 2004, Fitzgibbon *et al.* 2007). Depending on the size of the prey SDA varies and usually size of prey is a small percentage (1-3%) of the body mass (Secor 2008).

The total energy requirement is transformed from kinetic energy $4 \cdot \sqrt{E_k} t$. In this case we exclude the standard SDA for endothermic fishes i.e. 35% as an included energetic cost to the total energy requirement. SDA is only a temporarily increase in metabolic rate. Other energy costs e.g. from growth, excretion and reproduction is not considered in the present total energy requirement budget.

The total energy requirement $4 \cdot \sqrt{E_k} t$ in ($m^2 \cdot kg\ s^{-2}$) may be transformed to calories using a conversion constant (1 Joule = 0.239 calorie). The approximate minimum energy requirements per individual and the mass specific metabolic rate using the total kcal per day may be calculated to give an estimate. Moreover, 1 kcal increase the temperature of 1 kg muscle by 1.22°C which means the temperature (°C) may be established by dividing the kcal with the specific heat constant for muscles 0.82 kcal/kg °C^{-1} (Carey *et al.* 1982). The total heat production (e.g. kcal/M_{Total}(kg) h^{-1} or °C/M_{Total}(kg) h^{-1}) can be estimated for total mass (M_{Total}) in regards of body mass or trunk red muscles mass per time unit and likewise the mass specific heat production in kcal/kg · h^{-1} or in °C/kg · h^{-1} (Neil *et al.* 1976, Carey *et al.* 1982). However the heat loss is unknown for all size classes in the great white shark. Only the heat loss from a 4.6 m total length great white shark have been measured to 38.5 % (Carey *et al.* 1982) and may be used as a proxy when determining the estimated body core temperature near the red muscles for other size classes (Table 2.6.1). Total heat loss in small endothermic skipjack tuna *Katsuwonus pelamis* with a body mass ranging from 0.7 to 2.1 kg is 40.4-69 % where 22-31% could be accounted to the gills (Brill *et al.* 1978). This suggests the heat loss in endothermic fish have a limited size dependence and may be confounded to activity level as for instance a higher heart rate increases the amount of blood cooled in the gills.

Because the great white shark is a ram-ventilator constantly swimming the sustained swimming mode is the closest mode to resting (basal metabolic rate) or rather routine metabolic rate. This means the routine metabolic rate oxygen consumption per mass and time unit may be determined and plotted against pervious routine metabolic rate measurements for neonates (Ezcurra *et al.* 2012). Oxygen consumed during sustained swimming may be converted by, 3.36 cal is 1 mg O_2 (Carey *et al.* 1982) this will give the unit mg O_2/kg h^{-1}.

To estimate the total heat production (°C/TRMM h^{-1}) in trunk red muscle mass ($TRMM_\Delta$) the following expression (eq. 2.6f) was used. The total energy requirement $\left(4 \cdot \sqrt{E_k}\right) t$ and the resulting heat production (H_Δ) 75% was multiplied with the heat loss (H_∇) 38.5% and divided by the mass specific heat capacity for muscles 0.82 kcal/kg °C $^{-1}$ adopted from Carey *et al.* (1982). Heat loss would refer to the convection and conduction from the surrounding water and differ depending on water temperature.

Equation (2.6f)

$$\frac{\left(4 \cdot \sqrt{E_k}\right) t \cdot H_\Delta \cdot H_\nabla}{0.82} = TRMM_\Delta$$

The mass specific heat production for trunk red muscle mass (eq. 2.6g) was quantified by diving total heat production with trunk red muscle mass (kg). The mass specific heat production quantity was denoted with gamma (γ) to show the difference to the total heat production for trunk red muscle mass, which denoted with only delta (Δ).

Equation (2.6g)

$$\frac{TRMM_\Delta}{TRMM} = TRMM_{\Delta\gamma}$$

Mass specific heat production for stomach

The mass specific heat production in trunk red muscle mass during sustained swimming is given in (eq. 2.6g). However to increase the temperature to the recorded stomach temperatures (Lowe & Goldman 2001) the trunk red muscle mass must work at or close to no heat loss from the trunk red muscle mass to produce the heat recorded. Additionally specific dynamic action (SDA) will increase the metabolic activity. An equation is presented (eq. 2.6h) where $T_{S\gamma}$ (°C/kg h^{-1}) is the mass specific stomach heat production. This is calculated using (eq. 2.6g) adding tuna SDA of 35% additional metabolic activity (1.35) adopted from Fitzgibbon *et al.* (2006). Note SDA is not given a visceral mass, to simply the heat production is given via the trunk red muscle mass as the metabolic activity in the viscera probably is largely governed by the red muscle heat production (convection and conduction):

Equation (2.6h)

$$\frac{\frac{(4\cdot\sqrt{E_k t})\cdot H_\Delta \cdot SDA}{TRMM}}{0.82} = T_{S\gamma}$$

Statistical analysis

For numeric analysis of collected data, MS Excel (v. 14.2.0) was used. Data was checked visually for normal distribution. Regression analysis of allometric equation was done in MS Excel and AnalystSoft StatPlus:mac (Mac OS. v. 2009) to determine r^2 from scatter plots fitted to the allometric equation and the standard error for the scaling constant *a* and scaling exponent *b* after log transformation (2.6m).

A t-test (two-tailed) was used to test if there was a significant dependence of the allometric relationship between the variables via Pearson's correlation (eq. 2.6i): The t-test used ($\alpha = 0.05$) and the null-hypothesis ($H_0 = 0$, $b = 0$).

Equation (2.6i)

$$t = \frac{r\sqrt{n-2}}{\sqrt{1-r^2}}$$

The allometric relationship for slope *b* was tested in another t-test (eq. 2.6j) for isometry (*b* = isometric, $\alpha = 0.05$), which was the second null-hypothesis (H_i = isometric) dimension dependant on the variables tested. If the allometric relationship was not isometric, a differential growth of the dependant variable was evident which may be interpreted as being of biological significance. The

value of *b* was tested against different isometric values dependant on the dimension of the variables (e.g. H_i = 1 in size-on-size, H_i = 2 in area-on-length, H_i = 3 in mass-on-length). To test *b* against the null-hypothesis (H_i) the following t-test was used where SE_b is standard error for the slope *b*:

<div align="right">Equation (2.6j)</div>

$$t = \frac{b - H_i}{SE_b}$$

To investigate the standard error for the constant *a* and power exponent *b* from the non-linear allometric equation, it was log-transformed to create a linear equation:

<div align="right">Equation (2.6k)</div>

$$Log\ y = \log a + \mathrm{b} \log x$$

Linear regression analysis was done on the log-transformed equation (eq. 2.6k) to investigate the standard error (*SE*) of the scaling constant *a,* and of the scaling exponent *b, and is* presented as the standard error of mean (± *SE*).

3. RESULTS

3.1 Red muscles and heat production

Body length variation

There was a significant individual variation in fork length in great white sharks included in this study, resulting in the fact that longer individuals than anticipated were dissected and an additional 13th cross section was possible to cut due to the proximally 5% longer fork length in some great white sharks. This suggests South African great white sharks are longer compared to collected specimens in the North West Atlantic (Carey *et al.* 1985).

Position of red muscles

The red muscle area was greater below the dorsal fin and in cross sections 5-6 (fig. 5, fig. 3) compared to the rest of the cross sections for juveniles and sub-adults (*n* = 11) figure (5). In adults (*n* = 1) cross section 4 (fig. 5, fig. 3) had greater red muscle area. In the neonates (*n* = 6) the red muscle distribution was uniform while in other size classes the majority of the red muscles was positioned in the anterior part of the of the trunk indicating a rearrangement of red muscle position in the body as the great white shark increase in size. In two juveniles the red muscle area increased in the anterior transition of the caudal peduncle (cross section 9 and 11 in figure 3 and 5) to similar sized area found in the anterior parts (cross section 5-6).

Trunk Red Muscle Mass

The red muscle mass growth was isometric (H$_i$ = 1, *b* = 0.9723±0.0814 SE, *a* = 0.0308, *n* = 18) to the body mass growth (Table 2). Both neonates (*n* = 6) and juveniles (*n* = 8) have an increasing trend of trunk red muscle mass to body mass but those relationships were not significant. Large variation in trunk red muscle mass was noted for neonates and juveniles, but was not significant to

sex. The results show that neonates and juveniles have the largest proportion of trunk red muscle mass to body mass compared to sub-adults and adults. Neonates show an arithmetic mean of 2.6% trunk red muscle mass and juveniles an arithmetic mean of 3.3% trunk red muscle mass. The largest variation trunk red muscle mass occurs in juveniles spanning from 2.0-4.2%. Neonates span between 2.0-3.3% trunk red muscle mass. Sub-adults ($n = 3$) and adults ($n = 1$) show a small span of variation and lower arithmetic mean of 2.0% and 2.2 % trunk red muscle mass respectively (one adult only). This may be due to a small sample size of those large individuals ($n = 4$) and thus the decreased proportion in trunk red muscle mass from neonates and juveniles to sub-adults and adults may simply be an artefact of small sample size. Arithmetic mean for all size classes was 2.8% ($n = 18$). All specimens presented in appendix Table A1.

Swimming speed

The swimming speed for the great white shark of different sizes was calculated (fig. 13) via the swimming speed model validated by 63 fish species empirically tested (Sambilay 1990). The results show that neonates had the slowest burst and sustained swimming speeds while the adults had the fastest burst and sustained swimming speeds, which was expected (Sambilay 1990). The maximum sustained swimming speed for the largest ($n = 10$) great white shark (PCL 3.73 m) was estimated to 10.1 km/h (mean adults 9.3 km/h) and maximum burst swimming speed 58.6 km/h (mean adults 53.7 km/h). For sub-adults ($n = 50$) the maximum sustained swimming speed was estimated to 8.3 km/h (mean sub-adults 7.9 km/h) and maximum burst swimming speed 48.3 km/h (mean sub-adults 46.2 km/h). For juveniles ($n = 189$) the maximum sustained swimming speed was 7.7 km/h (mean juveniles 6.8 km/h) and maximum burst swimming speed 44.4 km/h (mean juveniles 39.4 km/h). For neonates ($n = 65$) the maximum sustained swimming speed was 6.2 km/h (mean neonates 5.7 km/h) and maximum burst speed 35.9 km/h (mean neonates 33.2 km/h). See appendix Table A2.

Heat production during sustained swimming

Using the sustained swimming speed (eq. 2.6d), to estimate the thermal energy in trunk red muscle mass the total heat production (heat produced above the ambient medium) per total trunk red muscle mass was determined per hour (Table 2, fig. 8). The total trunk red muscle heat production including 38.5% heat loss per hour in the great white shark is highest in the adult great white shark (PCL 3.73 m, BM 900 kg, TRMM 19.6 kg), up to 114.2°C/TRMM h^{-1} (fig. 8). For the same great white shark the mass specific heat production (Table 2, fig. 9) was 5.8°C/kg h^{-1} (including 38.5% heat loss) for trunk red muscles mass which is similar (5.0°C/kg h^{-1}) to measurements in Carey *et al.* (1982). The smallest great white shark per trunk red muscle mass (PCL = 1.47 m, BM = 61 kg, TRMM = 1.43) had a mass specific heat production in trunk red muscle mass of 11.1°C/kg h^{-1} including heat loss and total heat production in trunk red muscle mass of 15.8°C/TRMM h^{-1} (fig. 8) including heat loss indicating that neonates and juveniles produce up to 5.3°C/kg h^{-1} more heat per kilogram red muscles than adults (fig. 9) but show 98.2°C/TRMM h^{-1} less heat production in total trunk red muscle mass compared to adults (fig. 8). This means the neonates produce approximately twice the mass specific heat production in the trunk red muscles mass compared to adults (fig. 9) but have 7 times lower total heat production compared to adults as a result of lower total trunk red muscle mass in neonates. The heat production is thus proportional to the red muscle mass. The scaling coefficient was 11.81±1.1 (Table 2) indicating that this is the red muscle temperature (°C) for all great white sharks independent of body size if the heat loss is 38.5%. Without heat loss (38.5%) the red muscle heat production coefficient is 19.1 °C/kg h^{-1}. Neonates had a mean mass specific heat production in trunk red muscle mass of 10.5°C/kg h^{-1}. Juveniles had a mean mass

specific heat production in trunk red muscle mass of 7.9°C/kg h^{-1} and sub-adults 8.0°C/kg h^{-1} which is about the same but the gradual decrease in mass specific heat production is clearly shown in figure (9) according to the slope (b = -0.31). One adult had a mass specific heat production in trunk red muscles mass of 5.8°C/kg h^{-1}.

Mass specific stomach heat production was highest in neonates and lowest for adults (fig. 11). The scaling coefficient was 25.9±1.1 (Table 2) indicating that this is the stomach temperature (°C) for all great white sharks independent of body size. The scaling exponent which is the same for trunk red muscle mass (b = -0.31, Table 2) indicates that with increasing body mass the heat loss decreases; with 31% per kilogram trunk red muscle mass to sustain the stomach temperature of 25.9±1.1°C/kg h^{-1} (fig. 11). The lowest heat loss is found in the largest great white sharks and the heat loss is almost total for individuals with trunk red muscle mass below 2.5 kg (fig. 11).

Table 2: Results from allometric equations in this study. Results are shown with standard errors (SE) for scaling parameters and significance of H$_0$. If tested for isometry and significant (H$_i$) results are indicated by (Yes/No). TRMM, trunk red muscle mass, CFH, caudal fin height, CFA, caudal fin area, CFAR, caudal fin aspect ratio, PCL, precaudal length, Δ, difference from internal to ambient temperature, γ mass specific, BM, body mass, RMR, routine metabolic rate.

Dependant variable	Indep. variable	b	SE$_b$	a	SE$_a$	r^2	P H$_0$	Isometry	H$_i$	n
TRMM (kg)	BM (kg)	0.97	±0.0814	0.0308	±1.49	0.89899	P < 0.0001	Yes	1	18
CFH (mm) All	PCL (mm)	0.90	±0.0260	5.3761	±1.15	0.79443	P < 0.0001	No	1	314
CFH (mm) Neonate	PCL (mm)	1.02	±0.0840	0.2808	±1.86	0.70129	P < 0.0001	Yes	1	65
CFH (mm) Juvenile	PCL (mm)	0.75	±0.0978	2.0113	±2.11	0.24355	P < 0.0001	No	1	189
CFH (mm) Sub-adult	PCL (mm)	1.26	±0.1745	0.0393	±3.93	0.52214	P < 0.0001	Yes	1	50
CFH (mm) Adult	PCL (mm)	1.35	±0.4748	0.0173	±46.87	0.50570	P < 0.05	Yes	1	10
CFA (mm^2)	CFH (mm)	1.78	±0.1964	0.9223	±3.49	0.93243	P < 0.0001	Yes	2	8
CFAR	PCL (cm)	0.19	±0.0081	1.5636	±1.04	0.63795	P < 0.0001	No	1	314
Max. stomach volume (l)	BM (kg)	1.16	±0.1386	42.926	±2.08	0.95931	P< 0.0001	Yes	1	5
Burst speed (km/h)	PCL (cm)	0.68	±0.003	1.0041	±1.05	0.99477	P < 0.0001	No test	-	314
Sustained speed (km/h)	PCL (cm)	0.68	±0.003	0.1736	±1.01	0.99474	P < 0.0001	No test	-	314
TRMMΔγ (°C/kg h^{-1})	TRMM (kg)	-0.31	±0.064	11.8129	±1.10	0.63147	P < 0.001	No test	-	16
StomachΔγ (°C/kg h^{-1})	TRMM (kg)	-0.31	±0.064	25.931	±1.10	0.63147	P < 0.001	No test	-	16
TRMMΔ (°C/TRMM h^{-1})	TRMM (kg)	0.68	±0.064	11.8129	±1.10	0.88900	P < 0.0001	No test	-	16
BMγ (kcal/kg day^{-1})	BM (kg)	-0.28	±0.008	37.405	±1.04	0.98629	P < 0.0001	No test	-	16
Daily Energy (kcal/day)	BM (kg)	0.71	±0.008	37.405	±1.04	0.99777	P < 0.0001	Two tests	-	16
RMRγ (O$_2$ mg/kg h^{-1})	BM (kg)	-0.28	±0.008	380.36	±1.04	0.98629	P < 0.0001	No test	-	19

Daily energy requirement and routine metabolic rate

A 900 kg great white shark (PCL 3.63 m) has a daily caloric requirement of 4,871 kcal (fig. 17), and the mass specific daily energy requirement is thus 5.4 kcal/kg (fig 16). In comparison a 23 kg great white shark have close to three times higher mass specific daily caloric requirement of 15.3 kcal/kg (fig. 16) but only a total daily caloric requirements of 352.9 kcal (fig. 17). The scaling

exponent ($b = 0.71$) was tested in a two-tailed t-test (eq. 2.6j) for the resting metabolic scaling exponent (basal metabolic rate) for mammals in general ($b = 0.75$) and flying metabolic rate in bats and bird ($b = 0.72$) according to Schmidt-Nielson (1984) and found to he significant different to mammals in general ($P = 0.0002$) but not to birds and bats ($P = 0.3$). Routine metabolic rate is presented in figure (14) and model in Table 2. It fitted to previous measurements however showed the additional non-estimated metabolic activates to be 22-64% higher than the model for similar sized neonates measured in (Ezcurra *et al.* 2012) while the residual difference for adults using Carey *et al.* (1982) measurement for body temperature near red muscles converted to mass specific oxygen consumption was 1-2% (fig. 14).

3.2 Caudal fin allometry

Seven different relationships were investigated for caudal fin allometry. To investigate the ontogenetic differences during different life history stages, CFH were measured for each size class in the full sample population. For the 314 individuals investigated in the present study the allometric equations are presented in Table 2.

The ontogenetic development of the CFH (mm) to PCL (mm) showed a negative allometry ($b = 0.90$) for all size classes from neonates to adults (Table 2). However when tested for isometry for each size class the slope (b) demonstrated a significant negative allometry only for juveniles ($b = 0.75$, P<0.05, $n = 189$, $H_i = 1$) while the other classes demonstrated isometry. All four relationships (fig. 12) for TH to PCL were significant as relationships ($H_0 = 0$) for neonates to sub-adults (P < 0.0001) and for adults (P < 0.05). The relationships are presented in four allometric equations (Table 2).

A relationship for CFH (mm) and CFA (mm^2) was also investigated (Table 2) in order to estimate the caudal fin aspect ratio (eq. 2.6c). However in this case, the slope (b) was tested for isometry and found to be allometrically negative ($H_i = 2$, $n = 8$, P< 0.0001).

Caudal fin aspect ratio relationship was investigated (Table 2) and related to PCL (cm) showing an increase in the caudal fin aspect ratio, which may have ecological implications for inter-species comparison and food consumption per biomass (Paulomares & Pauly 1998). The t-test ($H_i = 2$, $n = 314$, P<0.0001) showed significant negative allometry for the CFAR ($b = 0.1904$).

3.3 Maximum stomach volume

For the first time, the stomach volume of the great white shark have been investigated and tested in an allometric equation. The results show isometric growth ($H_i = 1$, $b = 1.1662 \pm 0.1386$ SE) of maximum stomach volume related to body mass (fig. 15, Table 2), i.e. the stomach volume increase at the same rate as the body mass ($n = 5$, P< 0.0001, $H_0 = 0$).

4. DISCUSSION

4.1 Heat production and temperature effects

Position of red muscles

For all great white sharks except neonates the red muscle area increased more in the anterior part of the body (cross sections 1-6) compared (fig. 5) to the posterior part of the body (cross sections 7-12) during growth. This may indicate the red muscles have a higher potential to generate body core temperature in the anterior of the trunk where the stomach, gonads and suprahepatic rete are located. This part of the body is known to display regional endothermy and has the highest temperatures recorded (Lowe & Goldman 2001, Goldman *et al.* 1996, McCosker 1987).

Figure 5

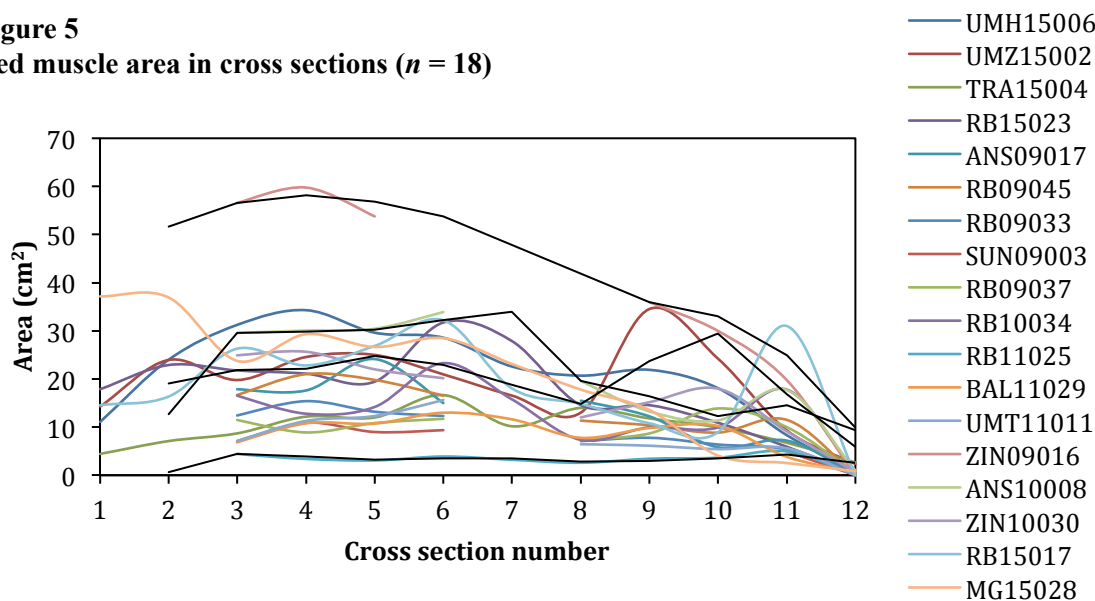**Red muscle area in cross sections (*n* = 18)**

Figure 5: The posterior area (cm^2) of trunk red muscle in the cross sections (1-12) per size class: neonate (RB11025, BAL11029, UMT11011, RB09037, SUN09003, TRA15004), juvenile (RB09033, RB09045, RB10034, UMH15006, UMZ15002, RB15023, RB15017, MG15028), sub-adult (ZIN10030, ANS10008, ANS09017) and adult (ZIN09016). In neonates the red muscles have a homogenous distribution while juveniles have a highly heterogeneous distribution. Sub-adults and adults have an anterior position of red muscles with fewer red muscles in the posterior part of the body. Black lines are moving average from below: Neonate (RB11025), juvenile (UMZ15002), sub-adult (ANS10008), and adult (ZIN09016). Note the larger amount of red muscles in the caudal peduncle (cross section 10) for the juvenile (UMZ15002).

The largest proportion of red muscles present in the anterior of the trunk (*n* = 18), was for that of a 900 kg female in cross section 4. Anterior location of red muscles are also noted for other thunniform swimmers (Graham *et al.* 1983) and suggests that the great white shark develop the thunniform swimming pattern during ontogeny. This is supported by the fact that neonate great white sharks investigated in this study have homogenous red muscle distribution throughout the body, suggesting that those muscles are poorly developed at birth. Juvenile great white sharks have the most heterogeneous red muscle distribution with great individual variation. Two juveniles show high distribution of red muscle in the caudal peduncle, in cross sections 9 and 11 (fig. 3, fig 5).
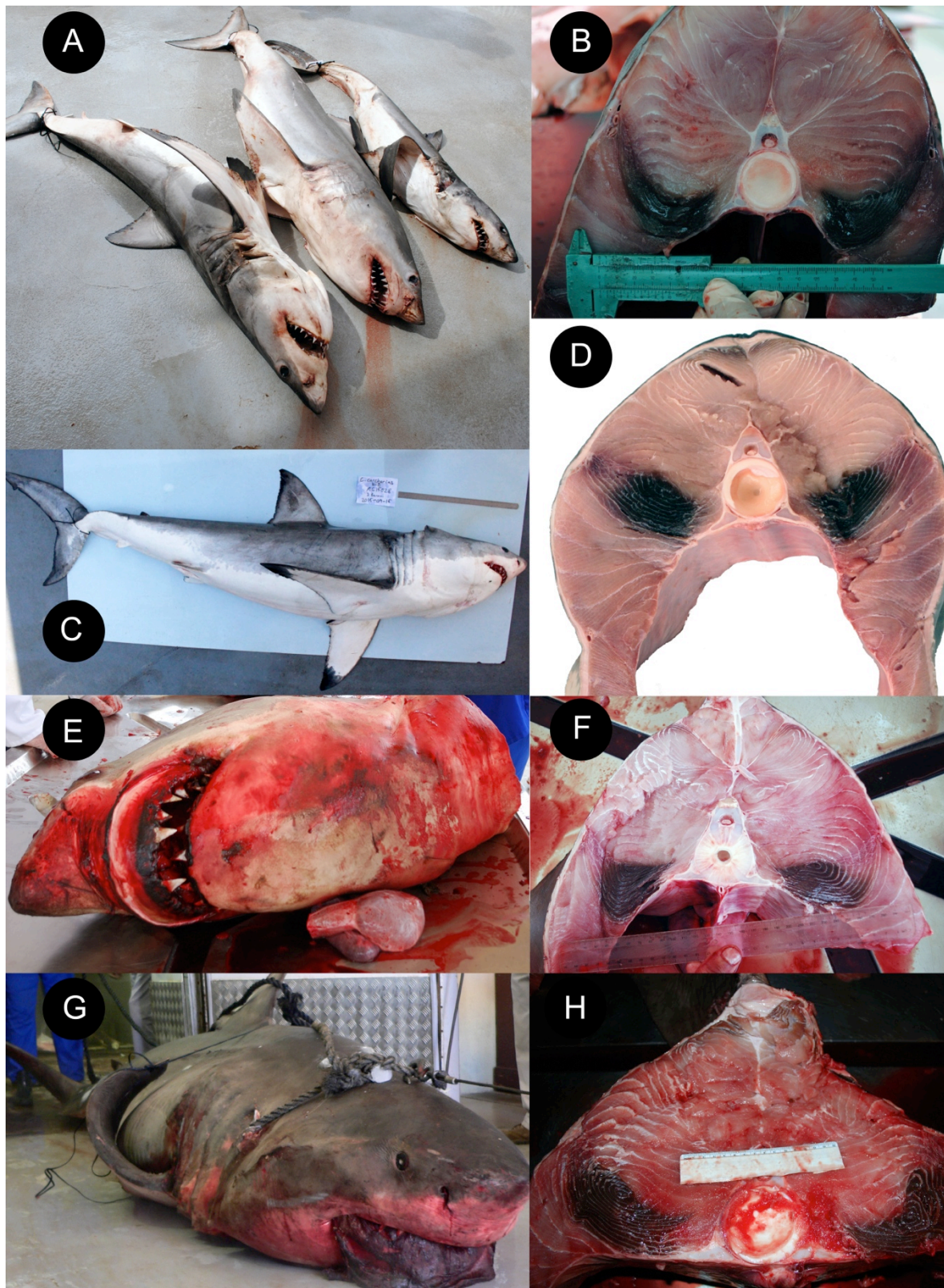
19

Figure 6: Life history stage showing cross section 5 in posterior view. A-B) Neonates from left to right (UMT11011, RB11025, BAL11029) with cross section from (UMT11011). C-D) Juvenile (MG15028). E-F) Sub-adult (ZIN1030). G-H) Adult (ZIN09016) a 900 kg female. For neonates, sub-adult and adult photo courtesy: Dr. Enrico Gennari.

The heat generated in the caudal peduncle through red muscles is likely dissipated via the large skin surface area, suggesting that those juveniles probably prefer warmer water temperatures, since red muscles are temperature sensitive in regards of power output in endotherm sharks (Sepulveda *et al.* 2015). However Lingham-Soliar (2005b) reported the caudal peduncle to contain thick layers of adipose tissue, the isolation efficiency of which has not been investigated may conserve heat in the caudal peduncle. Endurance of muscles in the caudal peduncle of juvenile great white sharks is feasible as a consequence of diet being mainly pelagic teleosts (Hussey *et al.* 2012).

Red muscles in the caudal peduncle also lose their central position and merge into a subcutaneous position (fig. 7). This is probably because of the increased skin surface area to muscle volume in the caudal peduncle likely result in limited ability to conserve heat generated in the red muscles. Dissections also show the caudal peduncle lacks well-developed *retia mirabilia*. In carangiform swimmers maximum red muscle proportion coincides with the greatest body flexure about 70% of the total length (Graham *et al.* 1983) as was the case for two juvenile great white sharks with high distribution of red muscle in the caudal peduncle, in cross sections 9 and 11, equivalent of 65% respectively 75% of total length (fig. 3, fig. 5).
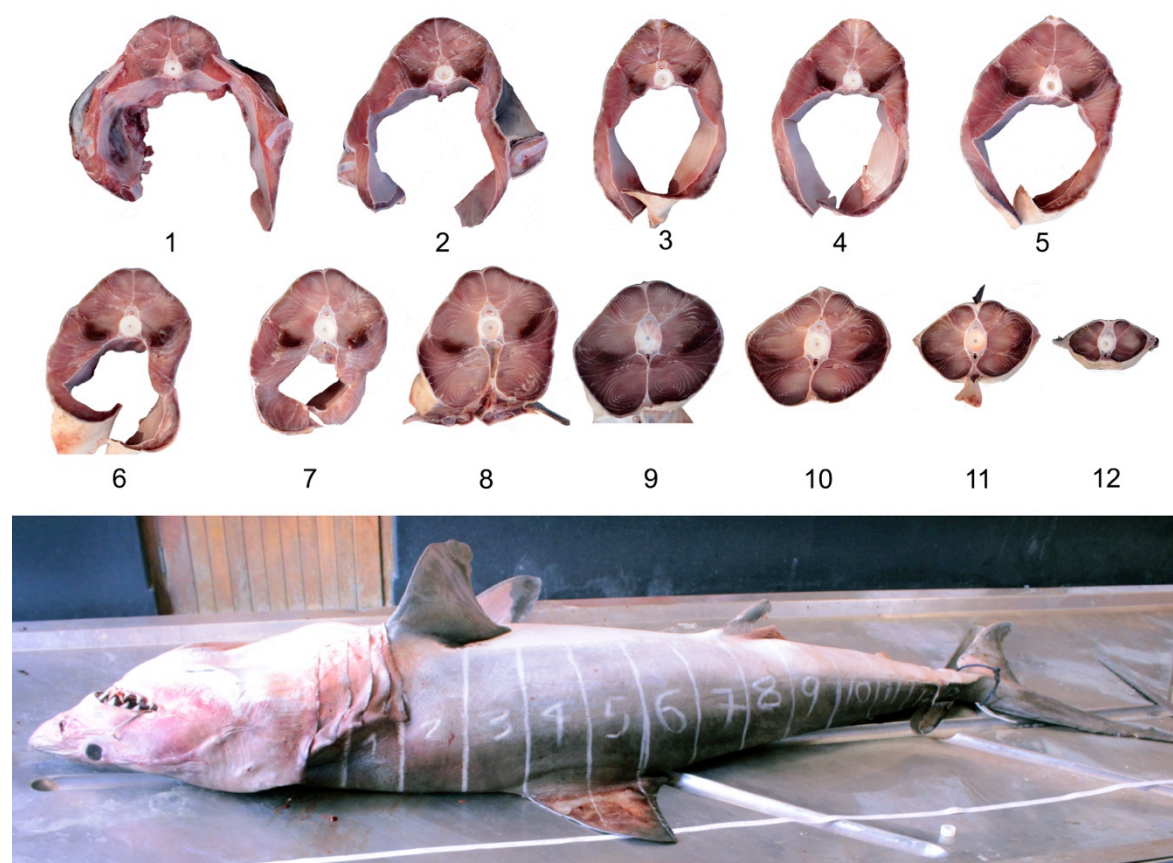

Figure 7: Trunk red muscle mass in 12 cross sections from a 158 cm (PCL) neonate male great white shark (TRA15004). Note the coloration of the epaxial musculature being pink rather than white. This suggests the muscle fibers have high myoglobin content. Red muscles are dark close to the centre of the body axis but merge this position in the caudal peduncle (cross sections 11-12) to the lateral sides. This part lack well-developed *retia mirabilia*.

Observations of pink muscles

Red muscles are slow twitching while white muscles are fast twitching (Syme & Shadwick 2011). Fishes that swim slowly have more slow moving muscles while fishes that swims fast have more fast moving muscles (Syme & Shadwick 2011). Great white sharks with the highest proportion red muscles would therefore be the most slow-moving individuals however this is not the case based on swimming speeds estimated in this study. Other muscles than only the red muscles must be used for sustained swimming. Pink muscle fibers are a skeletal muscle type not well studied and have been described as an intermediate tissue of red muscles and white muscles (Seamone & Syme 2015). Based on dissections in the great white shark the coloration varied between the red musculature close to the spinal column and the reddish musculature surrounding (fig. 7) indicating this musculature is pink. Carey (1982) observed this for various species of both lamnids and tunas.

However abdominal musculature has a paler colouration (fig. 7) than the epaxial musculature. In elasmobranchs two species have been studied and show pink musculature, namely the small-spotted catsharks *Scyliorhinus canicula* and the nursehound *S. stellaris*. Pelagic sharks have not been studied. In teleosts the pink muscles apparently supplement the red muscles during high speed (Coughlin & Rome 1996, Semone & Syme 2015) and have properties of fast twitching being moderately vascularised and show higher myoglobin contents than white muscles (Semone & Syme 2015). This indicate the pink muscles may be used to supplement the red muscles and possibly the red muscles play a role in warming the pink muscles to increase their efficiency. Wardle (1975) found muscle contraction time decrease with increased muscle temperature. If the great white shark has pink epaxial muscles (dorsal muscles), it would be able to gain swimming efficiency without overheating the red muscles. Heat from red muscles may be distributed in epaxial muscles through heated blood via parallel veins to the myosepta arranged throughout the epaxial musculature (Burne 1923). Histological examinations should investigate the epaxial pink muscles fibres further to determine their functions.

Proportion Trunk Red Muscle Mass to Body Mass

The trunk red muscle mass growth is isometric to body mass in the great white shark (Table 2) as reported for red muscle growth in both endothermic and ectothermic shark species (Bernal *et al*. 2003). Hence it follows the expected growth pattern of isometry for skeletal muscles (Bernal *et al*. 2003, Schmidt-Nielsen 1984) and do not increase proportionally more as the shark grows as of according to one observation in Carey *et al*. (1985). Nor does a change in the proportion trunk red muscle mass develop as the shark attains ontogenetic dietary shift at 3-3.5 meters total length or adult size, based on the data gathered in this study. In Bernal *et al*. (2003) data ($n = 4$) from Carey *et al*. (1985) was converted to percentage of red muscle mass of body mass using one cross section positioned at 50% fork length. Based on the results in this study (cross section 4) this is one of the cross sections showing the highest amount of trunk red muscle mass. By using this cross section Bernal *et al*. (2003) estimated a 3-6% proportion red muscle mass of body mass using data in Carey *et al*. (1985). This proportion red muscles mass is based on only one cross section with among the highest amount of trunk red muscles area explaining the rather high proportional estimate but the mean ($n = 4$) red muscle mass (Carey *et al*. 1985, Bernal *et al*. 2003) was 3.75% of body mass which is within the range of this study (2.0-4.2%, $n = 18$) and but higheter to the mean from this study (2.8%). In Bernal *et al*. (2003) five species of shark species investigated for red muscle

scaling was found to have red muscle proportion between 2.01-2.65% of body mass similar to current study.

Neonates and juveniles had the largest proportion of red muscles although the sample size for sub-adults and adults was small. Especially juveniles had large proportion of red muscles, which was not expected. However, juveniles also show a great variation with some individuals exceeding 4% trunk red muscles mass of body mass while others of similar size only have 2%. Based on the fact that red muscles produce heat it is reasonable to suggest that more red muscles increase heat production. Some juvenile great white sharks are thus more adapted to swim in colder waters having large amounts of red muscles. This does not necessarily indicate some juveniles are oceanodromous like adults (Boustrary *et al.* 2002, Bonfil *et al.* 2005, Weng *et al.* 2007) but migrate to different neritic habitats more frequently as noted for a total length 2.84 m female in Bonfil *et al.* (2005) moving between Mossel Bay in South Africa and southern Mozambique and expanded the niche from sub-tropic to temperate waters (Boustrary *et al.* 2002) in favour of increased prey opportunities. Increased red muscles amount will also increase swimming endurance.

Juveniles have on rare occasions been reported to scavenge on marine mammals (Dicken *et al.* 2013) and even occur at Seal Island, False Bay (Kock *et al.* 2013) were the water temperatures have on annual average show 12°C lower SST compared to KwaZulu-Natal (Smit *et al.* 2013). It is possible that the variation in red muscle proportion is a phenotypic phenomenon. Similar sized juveniles hunt prey in the colder waters of the Western Cape while other juveniles of the same size hunt in the warmer waters of the Eastern Cape. Nevertheless a genetic explanation is possible. An Atlantic population (Clade 2) and endemic easterly South African (Haplotype D) population have in fact been demonstrated (Andreotti *et al.* 2016) which, if genetic analysis were to be correlated for variation in red muscle morphology for similar sized juveniles, might explain the variability in red muscle mass. This would suggest there are one cold-water population and one warm water population of great white sharks in South Africa.

Neonate and juvenile great white sharks have a larger surface to volume ratio due to the surface rule (Schmidt-Nielsen 1984) and thus a higher capacity for heat loss compared to sub-adult and adult great white sharks. The proportionally larger red muscle mass to body mass in neonates and juveniles indicate that the red muscles in those size classes produce proportionally more heat. This is likely a result of the proportionally greater heat loss due to larger surface area to volume ratio.

Interestingly some juvenile great white sharks have a similar red muscle proportion as the albacore tuna *Thunnus alalunga,* having 4% red muscles of body mass (Dickson 1994). Red muscle proportion could reflect prey choice. Ambush-stalking behaviour observed for predatory activity around congregations of pinnipeds (Martin 2005, Klimley *et al.* 1996) do likely require large red muscles as a increased tolerance to the cold waters where this prey usually congregate. Temperature tolerance may be more efficiently gained by lower surface to volume ratio and proportionally larger trunk red muscle mass. The effect of red muscle heating is proportional to body surface-body volume ratio according to Kleiber's law (Kleiber 1932). The trunk red muscle mass is less than 5% of the body mass in all great white sharks examined (*n* = 18). Hence the epaxial pale muscles may work as a significant isolation for the red muscles thus preventing heat loss from conduction (Carey 1982, Bernal *et al.* 2003). Furthermore, based on observations in this study the liver may possibly provide ventral isolation from conduction, where the body wall is much thinner (Carey *et al.* 1985), while the counter-current systems retain heat in the blood system regionally by reducing cooling conduction by heating convection (Carey & Teal 1969).

Total heat production

The total heat production in the trunk red muscle mass during sustained swimming was approximately seven times higher for adults compared to neonates (fig. 8) indicating an ontogenetic difference in heat production capacity.

Heat production is proportional to the trunk red muscle mass that in turn is isometric to body mass according to results in this study (Table 2). This is clearly demonstrated in figure (8) showing neonates and juveniles producing between 15.8°C/TRMM h^{-1} in the trunk red muscle mass while the adult may produce at least 114°C/TRMM h^{-1}. Although the heat production in adults seems to be wrong we must not forget that the total heat production in large endothermic animals are high. If 114°C/TRMM h^{-1} is divided by 900 kg the heat production from the red muscles circulated in the body by the blood and distributed by tissue is only 0.12°C/kg h^{-1}. The increase in mass specific muscle temperature has been reported to be 0.15°C/kg h^{-1} for a similar sized adult (Carey *et al.* 1982). By transferring this heat to specific organs by increased heated blood flow to those locations within the body the tissue efficiency in those organs may increase 2-3 times due to temperature effects. The position of the red muscles also makes conduction to the body cavity highly likely. Organs in the body cavity may gain benefits from temperature effects.

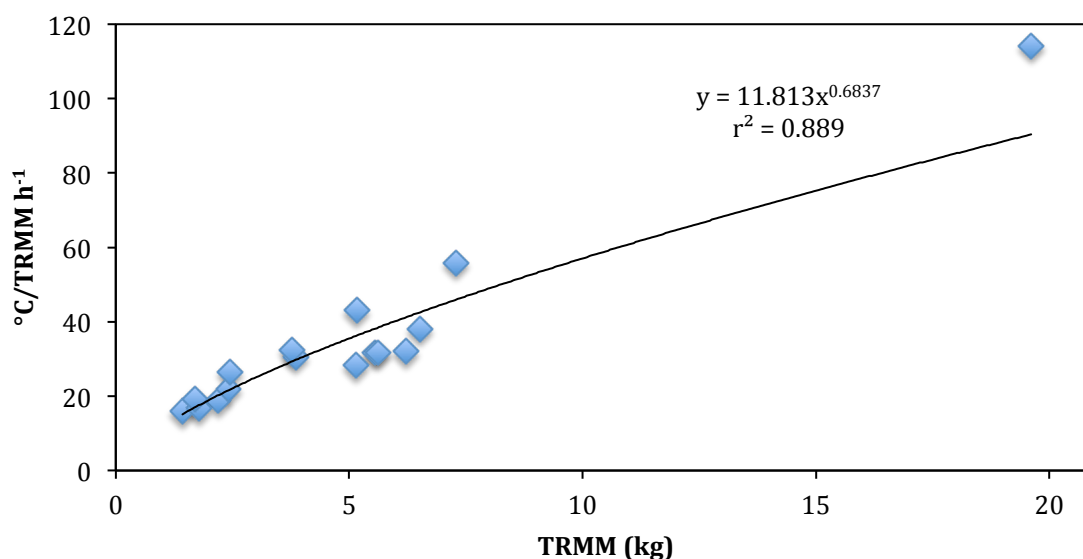**Figure 8**
Total heat production capacity in red muscles (*n* = 16)

$$y = 11.813x^{0.6837}$$
$$r^2 = 0.889$$

Figure 8: The total heat production capacity during sustained swimming in (°C/TRMM h^{-1}) for the trunk red muscle mass with heat loss (38.5%). Adults have approximately 7 times higher total heat production capacity than neonates, which indicate an ontogenetic difference in endothermic capacity. See Table 2 for details.

Mass specific heat production

The estimated temperature from allometric function (fig. 9) is close to previous field measurements (Tricas & McCosker 1984, Carey *et al.* 1982). Because we do not know the actual mass of the individuals from the field measurements it is hard to statistically test them against the slope. The estimate from this study is approximately 16-25% higher than the field measurements of muscle

temperature. However the results indicate that there is indeed a difference in endothermic capacity based on ontogeny in the great white shark.

The ontogenetic heat production is also dependant on the swimming speed. Field measurements (Tricas & McCosker 1984, Carey *et al.* 1982) recorded great white sharks that may have been changing swimming speed between sustained swimming and burst speeds. This means their muscle temperature would have risen and cooled dependant on muscle work. If there is a constant internal temperature and this temperature is achieved the shark will not need to produce more heat above the ambient medium than necessary. In the case of the shark repored by Tricas & McCosker (1984) the ambient water temperature was 21°C and the internal muscle temperature 24-25°C. For the shark in Carey *et al.* (1982) muscle temperature was 18-20°C and the ambient water between 14.7-16.7°C. Results in this study demonstrate the trunk red muscle mass varies between 2-4%, a factor of variation in field measurements as well. The proportion trunk red muscle mass is unknown from the great white sharks from field measurements (Tricas & McCosker 1984, Carey *et al.* 1982) and may vary 2-4%. Trunk red muscle mass had to be estimated in figure (9) from the allometric equation for red muscle proportion of body mass from this study (Table 2) and from body lengths converted to body mass using Mollet & Calliet (1996).

Figure 9
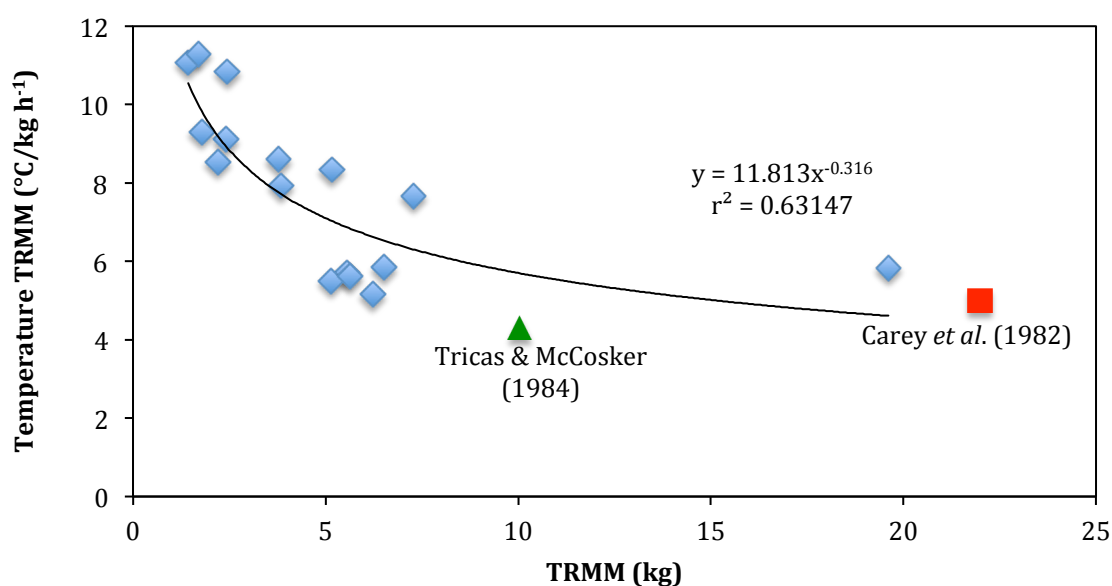**Mass specific red muscle heat production including heat loss (*n* = 16)**

Figure 9: The mass specific heat production with heat loss (38.5%) for red muscles in (°C/kg h^{-1}) with plotted data for temperature field measurements near or in the red muscles (Tricas & McCosker 1984, Carey *et al.* 1982). Field measurement are 4.3°C (Tricas & McCosker 1984) and 5.0°C (Carey *et al.* 1982) for a thermometer 30 cm deep into the musculature. Trunk red muscles mass estimated using red muscle proportion model from this study (Table 2) and from body mass using total length (Mollet & Calliet 1996).

The heat production is highest in neonates and decrease according to size (fig. 9), a corresponding heat production has also been observed in tunas (Kitagawa *et al.* 2006) where the smallest individuals show the highest heat production. In the great white shark the heat production in neonates is approximately the double found in adults. The scaling exponent in the great white shark (*b* = -0.31, fig. 9) is close to the inverse ratio of scaling in the surface rule (-0.33) and likely

indicate that as the great white shark grows the increased volume to ratio to decreasing surface area limits heat loss. However the heat in the inertia is similar for all size classes (fig. 9, Table 2). With heat loss the scaling coefficient (a) is 11.8±1.1°C/kg h^{-1} but without heat loss a = 19.1±1.8°C/kg h^{-1} and coincides with the mean sea surface temperature (SST) of young of the year catches from the North West Atlantic. The SST for neonates is 19.5±1.9°C and also measured muscle temperature (18-20°C) for an adult in the same temperature range (Curtis *et al.* 2014, Carey *et al.* 1982). This might indicate 19°C is the optimal temperature for neonates and that there is a temperature homeostasis for all size classes in regards of the red muscle temperature. Neonates likely have a total heat loss to the surrounding environment due to their small size. Adults are caught in colder SST waters 17.7±4.6°C (Curtis *et al.* 2014) and likewise the scaling coefficient with heat loss 11.8±1.1°C/kg h^{-1} (Table 2) may indicate an internal temperature. The lowest SST a great white shark was caught in measured 9°C (Curtis *et al.* 2014) added with the lowest heat production (10.7°C) from (Table 2) equals to a total internal temperature of 19.7°C. This is suggested to be the approximate internal red muscle temperature for the species based the results in this study (19.1±1.8°C/kg h^{-1}) excluding heat loss (38.5%). Previous observation of SST for neonates and juveniles (Dicken & Booth 2013, Dewar *et al.* 2004, Bruce & Bradford 2012, Curtis *et al.* 2014) together with measured muscle temperature in an adult (Carey *et al.* 1982) points out an optimal water temperature close to 19°C for great white sharks.

Heat transfer and temperature effects

Previous studies on endothermic fish have tried mathematically to estimate the heat production in tunas resulting in overheating (Brill *et al.* 1994, Sharp & Vlymen 1978, Neil *et al.* 1976). The overheating problem is especially true during high activity i.e. burst swimming. In Brill *et al.* (1994) cooling control from the central nervous system for blood flow was discussed to cope with the excessive heat. However, Kitagawa *et al.* (2006) found based on field measurements that the Pacific bluefin tuna *Thunnus orientalis* do not overheat and that the heat production decrease with increased body mass. This indicates the mass specific heat production becomes lower as the fish grows, a well-known phenomenon observed for the mass specific metabolic rate in mammals (Schmidt-Nielsen 1997). Furthermore yellowfin tuna *Thunnus albacares* can heat transfer, a function evolved to possibly to avoid overheating (Dewar *et al.* 1994). Based on the convergent evolution between lamnids and tunas (Bernal *et al.* 2001, Donley *et al.* 2004) it is assumed that similar heat transfer mechanisms have evolved in lamnids and the great white shark as reported for tunas (Dewar *et al.* 1994, Brill *et al.*1994). Heat production estimate in this study is based on that the trunk red muscle mass is used for propulsion. This indicate that the red muscle heat production during sustained swimming occurs in 2-4% of the body mass. The shark is suggested to regulate heat transfer by using different swimming muscles and by dispersing heated blood flow to those muscles to increase aerobic metabolism (Carey 1982). Other organs such as the central nervous system may also have an increased aerobic metabolism strengthen by the fact that the eyes and brain have a rete and a red muscle vein draining heated blood to sinuses in the neurocranium from the red muscles (Block & Carey 1985, Wolf *et al.* 1988, Alexander 1998). Burne (1923) also observed counter-current vascular systems other than the *retia mirabilia* in the epaxial musculature of the porbeagle.

If the red muscles are used during sustained swimming speed while the rest of the epaxial musculature and other organs are used to supplement the red muscles (Coughlin & Rome 1996, Stränger & Stobier 2001) as the red muscles are heating them, the swimming efficiency would increase (Carey 1982, Wardle 1975) and no overheating occur in the red muscles. In other words

the great white shark is suggested to heat transfer (Dewar *et al.* 1994). Observation in this study and pervious reports (Carey 1982) indicates the epaxial musculature may in fact have pink muscles containing high levels of myoglobin judging from their rather reddish or pinkish colour (fig. 7). Muscles with high myoglobin content will benefit from a higher temperature compared to white muscles (Carey 1982). A higher temperature would make it easier for myoglobin to deliver oxygen to the mitochondria within the muscles. Pink muscles have properties in-between white and red muscles and offer more dynamic propulsion than the slow moving red muscles or quick moving white muscles. Quick recovery from burst speed is possible if muscles used during burst swimming are heated above the ambient medium (Wardle 1975).

By using blood as heat transfer and heating a insignificant body part (<5% of body mass) with the use of convection its is significantly possible to rise the thermal inertia to an equilibrium above the ambient environment using limited isolation of a thermal gradients consisting of muscle tissue slowly being cooled by conduction (Neil *et al.* 1976). The blood is cooled through the gills and will lose all gained heat production from the body to the ambient water temperature by thermal convection (Carey 1982). However the *retia mirabilia* reduce heat loss in the red muscles using convection with up to 98.3% heat retention efficiency in tunas (Carey 1982). Conductional heat loss to surrounding body tissue from red muscles may be beneficial. Thereby the heat production from the red muscles increases the metabolic activity in other tissues that cannot sustain a higher temperature to the ambient environment without additional heating. Increased temperature affect the swimming speed by muscle contraction time (Wardle 1975). Surrounding body tissue to the red muscles i.e. the skeletal (pink) muscles are aided in oxygen consumption for their mitochondria. This will probably increase the swimming dynamics and occasionally offload work done by the red muscles, thus also avoiding overheating and limitation of slow swimming from slow twitching red muscles.

Heat loss due to conduction can only be reduced with increased workload in the red muscles, heat-transferring convection or by isolation. Assuming no isolation exists except a temperature gradient through the musculature, creating conduction isotherms at different depth of the muscles (Bernal *et al.* 2003), the workload (metabolic demand) in the red muscles must play an important role in temperature regulation. The red muscles are free from other epaxial musculature by myosepta and can work separately (Donley *et al.* 2004). If the red muscles do all swimming propulsion the temperature will increase in the red muscles due to their insignificant mass to body mass ratio and high metabolic demand. By having extremely small propulsion muscles compared to body mass with high endurance capacity deep in the interior of the body the great white shark may increase the heat production significantly in a limited area while retaining produced heat using *retia mirabilia*.

Dietary induced thermogenesis (specific dynamic action) and predation are important metabolic demands. However the metabolic requirements are very different for digestion and finding a prey in terms of organs used. Hence two different modes of heat transfer is suggested (fig. 10) based on the autonomic nervous system directing warm blood to different organs:

Fight-or-flight mode: Heat production is transferred to skeletal muscles and neurocranium. The heat production is directed to the rest of the body to warm it and increase tissue efficiency in organs important for predation but the organs themselves will also produce heat due to temperature effects (Q_{10}). Heat is transferred depending on metabolic demand via blood. The workload of swimming is divided between red muscles and epaxial muscles. The brain and eyes are warmed by blood from the red muscles to increase predation efficiency (fig. 10A).
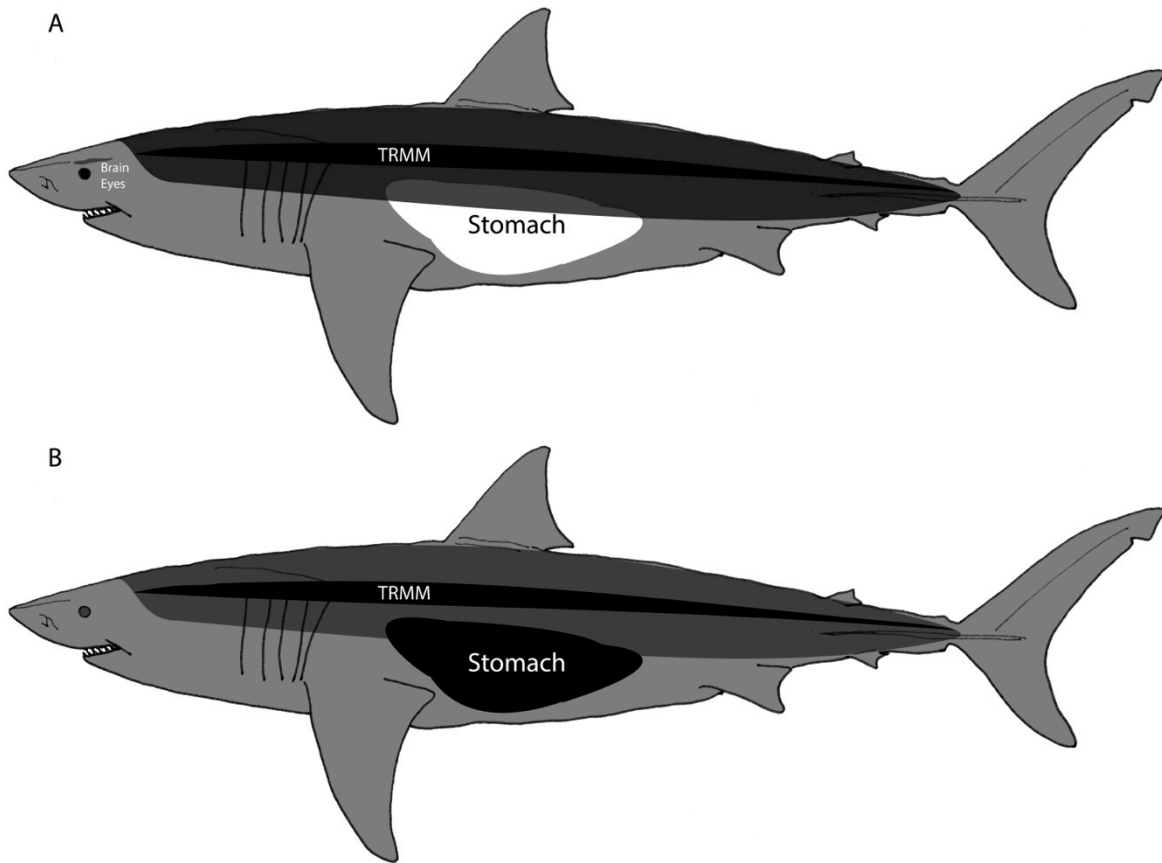
Figure 10: Heat transfer in the great white shark showing trunk red muscle mass (TRMM), brain, eyes and stomach: **A)** Fight-or-flight activity where heat production is concentrated to organs used for predation. In **B)** the rest and digest mode show the trunk red muscle mass generating heat which is transferred to the stomach instead of organs important for predation. Darker colours indicate higher temperature.

Rest-and-digest mode: Heat production in red muscles is transferred via blood to stomach and visceral organs to increase the digestion and assimilation efficiency. This will increase the temperature in the abdominal cavity via convection. Also conduction from red muscles may increase stomach temperature. Body parts with low metabolic demand and thus low amounts of blood will work as isolation from cooling conduction. As a consequence organs with low metabolic demand will become cooler and less efficient (fig. 10B) i.e. the larger mass of epaxial muscles.

The induced temperature effects of heat production imply the tissue efficacy may rise up to 2-3 times for every increase of 10°C in tissue (Schmidt-Nielsen 1997). The temperature effect (Q_{10}) plays a crucial role in the heat transfer mechanisms. This is especially true if the muscles have a high myoglobin content which can deliver up to 40% more oxygen per time unit to the mitochondria due to an increase in temperature of 10°C (Carey 1982). The haemoglobin levels of the blood is the same or higher than found in mammals and tunas indicating high oxygen carrying capacity (Emery 1985). In porbeagle the haemoglobin carrying capacity is temperature independent (Carey 1982). High blood pressure may reduce cooling conduction through heating convection. The heart of the great white shark is large with a ventricle of similar shape and thickness found in mammals and birds indicating high blood pressure (Emery 1985). High blood pressure is a characteristic of endothermy and high metabolic demand.

Stomach temperature

The stomach temperature in the great white shark has been reported to be 7-9°C and up to 14°C above ambient water temperature (Goldman *et al.* 1996, McCosker 1987). This is only possible if the red muscles can contribute to the same temperature. This is probably done by the red muscles increasing in heat production resulting in the same temperature level reported for the stomach. Alternatively the stomach has to produce heat above that of the red muscles using the supraheptic organ and visceral organs and in turn become cooled by the red muscles placed above the abdominal cavity having a lower temperature. The second scenario is highly unlikely.

The temperature reported in (fig. 9) is only based on heat produced in the trunk red muscle mass from sustained swimming excluding specific dynamic action (SDA). If the great white shark has satisfied the energy requirements after predation it will have to focus on digestion and rest i.e. the shark will enter into a "rest-and-digest"-mode and leave a "fight-or-flight"-mode. This means that organs such as brain, eyes and the large epaxial swimming muscles do not need to be warmed in the same manner as during predation. Furthermore, the specific dynamic action, also known as dietary induced thermogenesis will increase. The specific dynamic action is unknown in the great white shark but has been studied in another endothermic fish species, the southern bluefin tuna *Thunnus maccoyii,* showing an average specific dynamic action of 35% (Fitzgibbon *et al.* 2007). It is likely the great white shark also have a high specific dynamic action as an endothermic fish species. Demersal elasmobranchs have a specific dynamic action between 6-17% while teleosts in general show a variation between 15-20% (Carlson *et al.* 2004). If the specific dynamic action from the southern bluefin tuna (35%) is adopted for the great white shark and the propulsion is done only through the trunk red muscle mass (sustained swimming) with only insignificant cooling occurring from the emitting heat to the stomach, the mass specific temperature will resemble the levels reported for stomach temperature above ambient water temperature for all individuals (fig. 11) and reach reported stomach temperature of approximately 26°C (Lowe & Goldman 2001, Goldman *et al.* 1996, McCosker 1987).

Figure 11
Mass specific stomach heat production (*n* = 16)

$$y = 25.931x^{-0.316}$$
$$r^2 = 0.63147$$

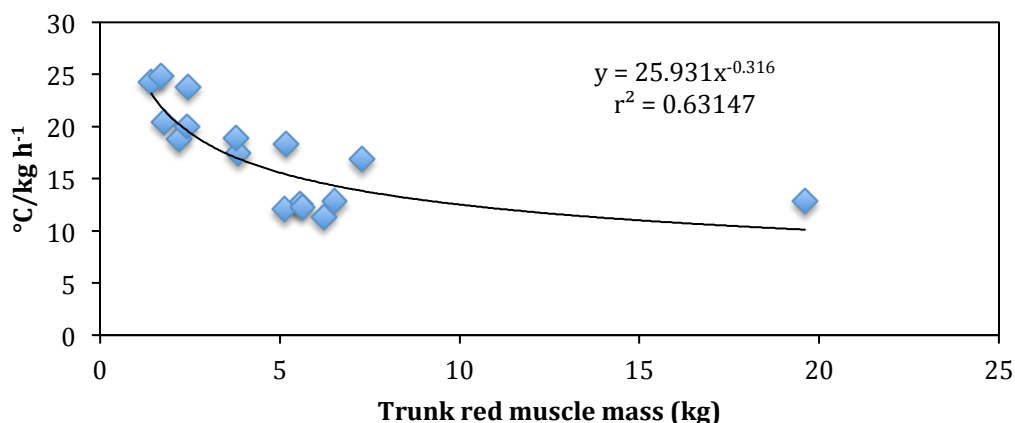**Figure 11:** The mass specific stomach heat production (°C/kg h^{-1}) plotted against trunk red muscle mass (kg) show that large great white sharks have a trunk red muscle mass of approximate 20 kg and may increase the temperature to 12.7°C/kg h^{-1} while neonates having a trunk red muscle mass of approximate 1.5 kg may produce up to 24.3°C/kg h^{-1} which is similar temperature observed in field measurements.

The scaling coefficient is 25.9±1.1°C (fig. 11, Table 2) indicating this is the stomach temperature independent of mass. The heat production is decreased by about a third as the great white shark increase in trunk red muscle mass. This is related to the surface rule inversed (-33%) indicating 31% lower heat loss per kilogram red muscles as a result of increased red muscle volume to the ratio decreasing surface area.

The maximum time to increase a full stomach of water above the ambient water temperature may also be calculated and gives an indication of the total time frame of digestion. One kcal increases 1 litre water 1°C. For a great white shark of 900 kg the time to heat the stomach volume (119.6 litres) of water to 12.7°C above ambient is 6.1 hours. The total heat production of the trunk red muscle mass generated in one hour with SDA is 250.6°C (excluding heat loss) but this will be absorbed by the stomach contents. This means no overheating occurs. However the full stomach of water having temperature 12.7°C needs to be heated with an effective heat production of 1,518.9°C to reach 12.7°C above ambient temperature. This is possible in 6.1 hours for a 900 kg great white shark and for smaller individuals (61 kg) it will take 3.6 hours to increase a 5.18 litre stomach volume. Note that the heat production is for several hours and the extrapolation use water with no external heat loss. If the shark would swim to warmer waters or consume a prey with high temperature the heating would be faster. Likewise the heating time will increase if the shark swims in colder waters and increase heat loss.

The time of heating for the stomach is proportional to the trunk red muscle mass. A juvenile great white shark (126 kg) having 4% trunk red muscle mass will only need 2.3 hour to heat a 12 litre full stomach while an individual having approximate half of this in trunk red muscle mass but the same stomach volume will need 4 hours, two times more time to heat the stomach. Considering the estimates are based on maximum stomach volume and the sharks probably only consume 1-3% of their body weight at any time (Secor 2008), the actual heating time of the stomach will be much faster. Maximum stomach volume equals maximum heating time (100% heating time). If for example a great white shark of 900 kg consumes a 9 kg prey of density similar to water e.g. an ectothermic fish, it will only take 3-4 minutes to heat the fish to the expected stomach temperature of 12.7°C above the ambient water temperature i.e. reaching ca. 26°C stomach temperature. In conclusion the trunk red muscle mass is proportional to time of digestion and assimilation. For a few juvenile great white sharks examined in this study showing up to 4% trunk red muscle mass probably use this phenomenon favourable to increase in growth faster by increased efficiency in specific dynamic action. Juveniles with larger trunk red muscle mass may consume more prey and convert the energy to growth faster than individuals in the same water temperature and of similar size with less trunk red muscle mass.

If stomach temperature is homeostatic at 26°C for the great white shark independent of body mass then the stomach heating could be a limiting factor for how large prey that is possible to heat in the stomach. If the mass specific heat production is 13°C and the shark have a stomach temperature of 26°C then it may take too much time to digest and assimilate large prey in cold waters. If there are enzymes or bacteria working within a narrow temperature interval for digestion and assimilation (26°C) then size of prey ingested and ambient temperature may be limiting the great white sharks ability to sustain the energy needs. This in turn could be a limiting factor for a temperature distribution for the species. If the ambient water is too cold and the shark has full stomach contents the shark will not be able to digest the prey consumed and thereby not sustain the energy

requirements until stomach content is digested. The size of ingested prey increases the energy needed for stomach heating. This offers an explanation for stranded great white sharks with full stomach contents in cold-water areas (Marin 2004).

4.2 Caudal fin allometry and habitat use

Considering the great white shark is a ram-ventilator and constantly needs to swim, the caudal fin has a central part in this animal's physiology in regards of heat produced. By constantly swimming the red muscles are constantly at work generating heat. Red muscles are slow moving at elevated heat levels (Carey 1982, Bernal *et al*. 2015, Carey *et al*. 1982), if they were to be cooled they would work even slower (Syme & Shadwick 2011). Muscle failure e.g. through starvation would lead to less heat production in the red muscles and subsequent cooling, resulting in even slower swimming thereby disrupting the oxygen supply, which in turn could lead to death by sinking.

The allometry of the caudal fin height have been investigated before (Lingham-Soliar 2005a) and showed negative allometry to fork length ($b = 0.78$, $n = 56$). In the current study there was also a negative allometric relationship for all size classes using the more reliable measurement precaudal length to caudal fin height (CFH) where ($b = 0.9$, $n = 314$, Table 2). However the caudal fin height was isometric for all size classes except juveniles (Table 2). Most of the great white sharks caught by KZNSB are juveniles; hence the relationship is skewed towards the negative allometry for this size class in the model for all size classes (Table 2).

The lower growth rate of the caudal fin height in juveniles indicates that the body length (PCL) grows faster than the caudal fin (Table 2). The fins consist of tissues such as cartilage and collagen-fibers (Lingham-Soliar 2005b), which are expected to have a slow growth rate compared to skeletal muscles and thus the length of the shark. This implies that the body length of juvenile great white sharks has a more rapid growth rate compared to neonates, sub-adults and adults. This is probably associated with more active feeding behaviour in juveniles and a result of abundance in neritic habitats. High abundance of juveniles has been found in neritic areas with high prey density of the Eastern Cape in South Africa (Dicken & Booth 2013). The neritic habitat of the Cape West Coast in South Africa is characterized by the nutrition rich cold upwelling Benguela Current while the warm Agulhas Current occurs offshore on the South African East Coast (Blamey *et al*. 2014). Although the Cape West Coast show nutrition rich cold upwelling most sub-adult and adult great white sharks observed are confined to the Southwest Coast of the Western Cape between Mossel Bay and False Bay where a majority of the Cape fur seal colonies are located (Cliff, personal communication, 2016). There is very few or low abundance of great white sharks in the Cape West Coast even though this is a high productive environment populated with Cape fur seals. This could however be biased by low human population (Cliff, personal communication, 2016). Juvenile great white sharks show a higher abundance in the Eastern Cape with over 96% being juveniles or neonates in Algoa Bay (Dicken *et al*. 2013, Dicken & Booth 2013) and catches from the KZNSB beach protective nets and experimental drumlines in this study ($n = 314$) show that 80% of the individuals are juveniles or neonates and only 3% adults along the KwaZulu-Natal coast. Adults and sub-adults show lower abundance and is thereby a limited threat to neonates and juveniles in the Eastern Cape. This spatial body size distribution between the Eastern Cape and the Western Cape where sub-adult and adult great white sharks are more abundant in the Western Cape indicate juveniles are confined to a neritic life-style in the Eastern Cape. A neritic life-style should favour more red muscles and a higher heat production as found in some juveniles in this study especially if their temperature

tolerance increases during ontogeny. Furthermore warm areas that occur in the surf zone within the neritic should be beneficial for growth. Great white sharks have been found to utilise this area during spring and summer months when sharp thermoclines are frequent (Dicken & Booth 2013, Kock *et al.* 2013, Blamey *et al.* 2014). Travelling offshore to warmer waters is likely to be a costly option compared to staying in the surf zone of the warm waters. In particular, adult female great white sharks have been found to occupy this area during summer months in Western Cape (Kock *et al.* 2013). There may be a trade-off between swimming in warm oceanic waters and the cold neritic waters where the cost of finding food is lower. The surf zone may be of particular interest for great white sharks as a digestion area due to warmer water temperatures, especially for neonate and juvenile great white sharks showing lower aspect ratio and less red muscle mass compared to adults (Table 2, fig. 8, fig. 9). Preferred prey consisting of pelagic teleosts (Hussey *et al.* 2012) is also present in high abundance of the neritic zone where juveniles are observed (Dicken & Booth 2013) and caught. According to stable carbon isotope data (Hussey *et al.* 2012) juveniles are more neritic than, sub-adults and adults that coincide with caudal fin data in this study.

Caudal fin aspect ratio (CFAR) between 4.5-7.2 is considered to correlate to a thunniform swimming mode (Sfakiotakis *et al.* 1999). Fish that show lower aspect ratio than 4.5 is regarded as presenting a carangiform or anguilliform swimming mode (Sfakiotakis *et al.* 1999). This is because high aspect ratio correlates to a high caudal fin area (CFA) and induces less drag per thrust produced (Sfakiotakis *et al.* 1999). The aspect ratio above 4.5 appeared in great white sharks from a 2.24 m precaudal length (large juvenile) and reached 4.99 for a 3.63 m precaudal length adult. This indicate that the aspect ratio associated with a thunniform swimming mode appear in sub-adults or the very largest juveniles. Juveniles and neonates have a lower aspect ratio, with the smallest 1.24 m precaudal length neonates having an aspect ratio of 3.48 and therefore present a carangiform swimming mode. Due to the obvious thunniform specialisations in the great white shark a better definition for the less developed aspect ratio in neonates and juveniles would be sub-thunniform swimming mode, rather than carangiform swimming mode. The position of trunk red muscle mass also confirms this less developed swimming mode (fig. 3, fig. 5, fig. 6, fig. 7), especially in neonates where this musculature is uniform through the body while adults have an anterior postion of red muscles. Thunniform swimming is developed during ontogeny.

Adult and sub-adult great white sharks are capable of trans-oceanic migration behaviour being oceanodromous (Weng *et al.* 2007, Bonfil *et al.* 2005, Boustany *et al.* 2002). Higher aspect ratio (Table 2) results in better lift performance and thus more efficient swimming. Consequently high caudal fin aspect ratio results in energy conservation, which is beneficial for long distance migration in oceanic habitat. The lower aspect ratio in neonates and juveniles may indicate that they are adapted for a life-style in the neritic zone. In this study, neonates and juveniles are also shown to have a higher variation in proportion of red muscles (fig. 5). Red muscles are used during slow swimming. A neritic life style yields less thunniform swimming and should be characterised by multiple turning behaviour (Sfakiotakis *et al.* 1999), which is easier during slow swimming and in a topographic habitat. Thunniform swimmers should have the red muscle mass in the anterior part of the trunk. Neonates have a uniform distribution and juveniles a heterogeneous distribution while sub-adults and adults have an anteriorly polarised distribution as found in tunas (fig. 5).

Figure 12
Caudal fin height allometry in four life history stages (*n* = 314)
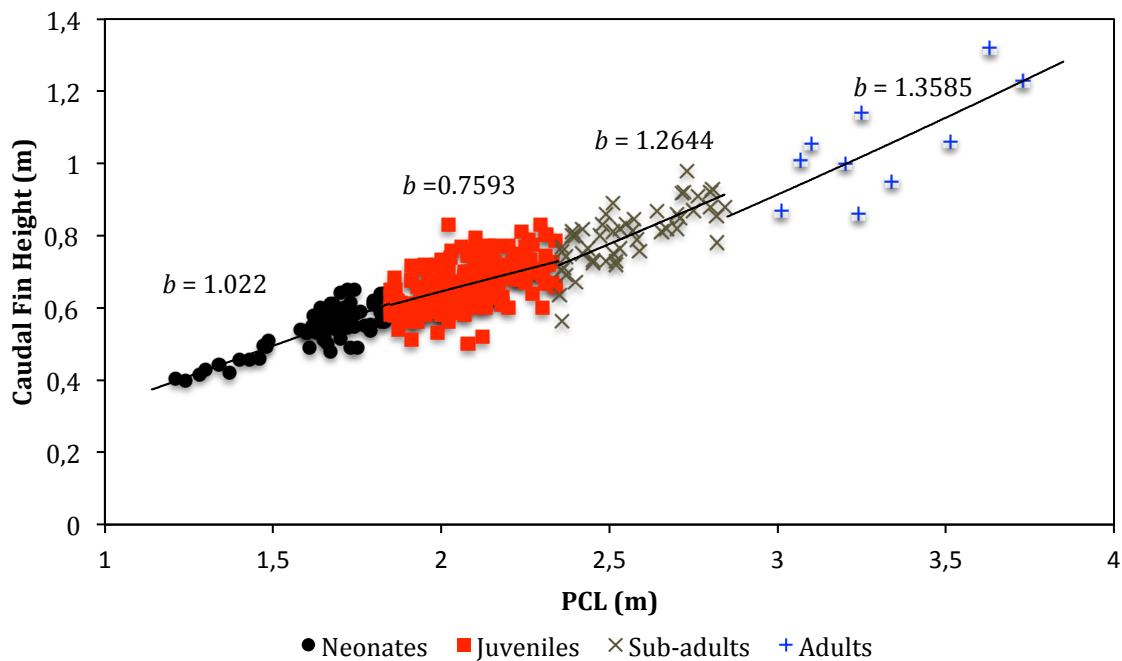

Figure 12: Showing the growth rate of caudal fin height (CFH) in meters and body length in precaudal length in meters (PCL) in four different life stages (*n* = 314). Only juveniles show a significant negative allometry, while other size classes have an isometric growth.

Remarks on body length measurements

There was a notable proportional length difference in fork length in some individuals examined. This morphological difference could be investigated with genetic examination to discriminate between genotypic or phenotypic explanations. There are two distinct genetic populations of great white sharks in South Africa (Andreotti *et al.* 2016) and the specimens described in Carey *et al.* (1985) were all from the North Atlantic genetically separate to South Africa (Andreotti *et al.* 2016, Gubili *et al.* 2010). The vertebral column in great white sharks has also been reported to vary in count of precaudal vertebral centra (100-108) between different geographical locations (Compagno 2001), which may advocate for further morphological examinations correlated to genetic studies of great white sharks populations.

4.3 Swimming speed and metabolic rate

Burst and sustained swimming speed

For the first time, in the present study, the swimming speed of the great white sharks have been modulated, based on methods described by Sambilay (1990). The mean sustained swimming speed for adults in this study (9.3 km/h) is similar to the observed. The mean swimming speed of twelve adult great white sharks (10.5 km/h) was reported in Semmens *et al.* (2013). The swimming speed observations done by Semmens *et al.* (2013) are based on active predatory behaviour in neritic habitat around pinnipeds colonies. Burst speed and sustained swimming speed could be measured

separately (Semmens *et al.* 2013). During oceanodromous migration, the swimming behaviour is different and the speed is slower. Tracking speeds are recorded to 2.2-5.4 km/h (Bonfil *et al.* 2010, Weng *et al.* 2007, Carey *et al.* 1982). According to Del Raye *et al.* (2013) this is the result of conserving energy via the use of drift diving behaviour. Drift diving and sinuous swimming reduce the mean swimming speed considerably, making migration-swimming speed underestimated (Del Raye *et al.* 2013, Weng *et al.* 2007). As a result the actual swimming speed from a great white shark using telemetry is hard to estimate. The swimming speeds from tagging studies are underestimated according to Weng *et al.* (2007). Ocean currents may also influence swimming speed measurements.

Observations in Semmens *et al.* (2013) indicate that the estimated burst speed in this study may indeed correspond to the real velocity. The great white sharks observed breaching at Seal Island in False Bay are juveniles and sub-adults (Kock *et al.* 2013, Martin *et al.* 2005, Fallows *et al.* 2012). Those great white sharks breach up to 2.4 meters above the surface (Martin & Hammerschlag 2012), why burst speed must be considerably higher than the average swimming speed. Based on calculations using observed height above water surface, angle from water surface and trajectory acceleration, and the gravity coefficient, the great white sharks are estimated to reach an initial velocity of 35 km/h (Martin & Hammerschlag 2012). The in water burst speed was estimated by Martin & Hammerschlag (2012) to 42.8 km/h based on video-recordings for a 3.4 m total length great white shark. The mean maximum burst speed for sub-adults was estimated to 46.2 km/h and for juveniles 44.4 km/h in this study. The burst velocity in the present study is thus slightly overestimated (by 3.4 km/h) according to Martin & Hammerschlag (2012). Alternatively, the full burst speed is not used during observations, currents obstruct swimming speed, or size estimates in the present study are different to those observed in Martin & Hammerschlag (2012). The most realistic explanation is probably that the great white sharks do not always use their maximum burst capacity. A tendency to avoid excessive energy during breaching towards towed seal-shaped decoys may be a confounding factor in the great white sharks behaviour overseen in pervious studies (Marin *et al.* 2005, Martin & Hammerschlag 2012, Fallows *et al.* 2012). High breaching may result in less manoeuvrability, which in turn would favour reduced burst speed and lead to lower breaching heights. Cape fur seals have an advantage in agility towards the great white shark (Martin & Hammerschlag 2012). Further research on breaching heights would help examining the burst speed to resolve the accuracy of the estimation in this study.

A mako shark dissected by the author caught by the KZNSB was also tested for the swimming speed model presented by Sambilay (1990). The caudal fin aspect ratio (CFAR = 5.89) from a precaudal length 1.92 m mako shark exceeded that of a precaudal length 3.73 m adult great white shark (CFAR = 4.92). The same great white shark had an estimated burst speed of 58.64 km/h while the mako shark had an estimated burst speed 41.39 km/h. The estimated sustained swimming speed for the same mako shark was 7.15 km/h, which is similar to reported velocity (Sepulveda *et al.* 2004) being 6.7±1.2 km/h for smaller individuals (FL 0.8-1.45 m). By implication, the great white shark may outswim the mako shark under certain circumstances. Mako sharks have also been confirmed, by stomach contents, to be prey of the great white shark (Postel 1958).

Known prey species of the great white shark such as bottlenose dolphin *Tursiops truncatus* reach a top speed of 40.3 km/h and the long-beaked common dolphin *Delphinus capensis* reaching 24.1 km/h (Rohr *et al.* 2002). This makes some dolphin species more susceptible as prey than others. In regards of pinnipeds the California sea lion *Zalophus californianus* may reach 9.4 km/h (Williams 1999) while the Cape fur seal reach 10 km/h (Costa *et al.* 2010) and the grey seal *Halichoerus*

grypus 10.8 km/h (Gallon *et al.* 2007) being in comparison to dolphin speed more accessible prey. Even neonates reach a burst speed of 33 km/h according to the results in this study. Although seals may be far slower swimmers than dolphins and therefore easier to catch, seals are also a lot more agile, which means the great white shark has to ambush seals and cannot rely on out swimming them. Furthermore, contrasting marine mammals with pelagic teleosts, the yellowfin tuna *Thunnus albacares* may reach 111 km/h and the mackerel 64.8 km/h *Scomber scombrus* (Sambilay 1990), thus exceeding the maximum speeds of the great white shark, unlike the swordfish *Xiphias gladius* reaching 40 km/h (Sambilay 1990). Swordfish has been reported as stomach contents in the great white shark (De Maddalena & Zuffa 2009, Fergusson 1996). In terms of speed it is therefore energetically beneficial to prey on slow moving blubber rich marine mammals rather than fast moving teleosts as the great white shark may have an advantage.

Figure 13
Modulated burst and sustained swimming speed (*n* = 314)

Burst swimming speed
$y = 1.0041x^{0.6858}$
$r^2 = 0.99477$

Sustained swimming speed
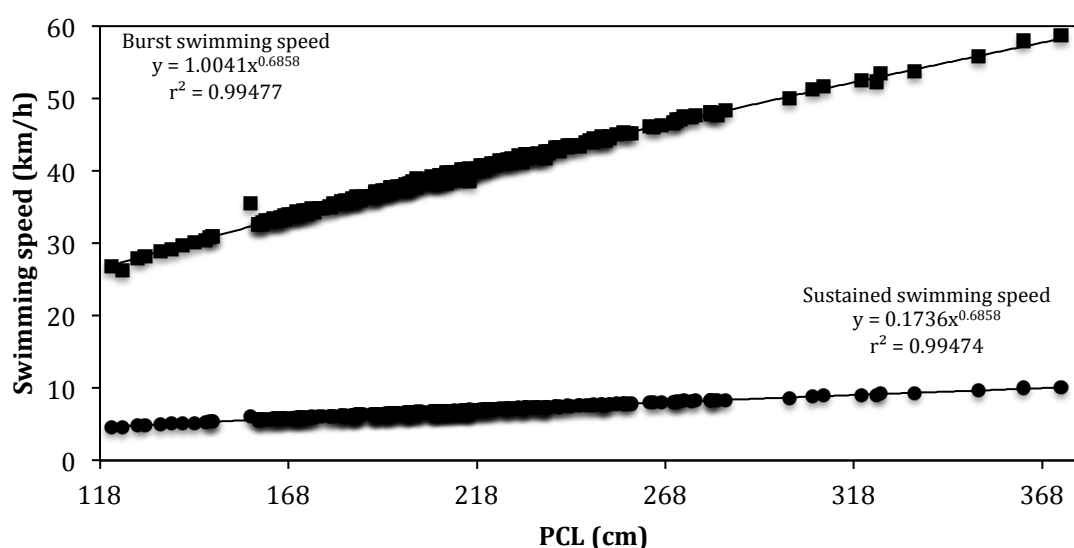$y = 0.1736x^{0.6858}$
$r^2 = 0.99474$

Figure 13: Estimated swimming speeds in great white sharks using caudal fin aspect ratio (CFAR) and precaudal length (PCL) in the swimming speed model (eq. 2.6d).

Routine metabolic rate using sustained swimming speed

Neonate routine metabolic rate have been measured in captivity (Ezcurra *et al.* 2012) and Carey *et al.* (1982) estimated the mass specific oxygen consumption for a 4.6 total length great white shark from temperature in the muscles. The routine metabolic rate was also estimated for swimming muscles (fig. 14) using the swimming speed shown in figure (13). This methodology fits approximately data points from Ezcurra *et al.* (2012) and Carey et *al.* (1982). The measurements of oxygen consumption for neonate great white sharks held in captivity during transport in Ezcurra *et al.* (2012) are higher than the estimates in this study (fig. 14). The results of the current study presents a new indirect method to estimate metabolic rate from sustained swimming speed rather than directly measure oxygen consumption from specimens held in captivity. Oxygen consumption difference (22-64%) in similar sized neonates (23-25 kg) may indicate additional residual metabolic activity not estimated for using only swimming speed to modulate routine metabolic rate.

Neonate measurements from Ezcurra *et al.* (2012) in figure (14) are higher than the allometric model predicted in this study. This may be because the sharks in Ezcurra *et al.* (2012) are held in

captivity and would experience increased stress. Also the temperature in captivity was 15°C (Ezcurra *et al.* 2012). This temperature may be colder than what neonates would normaly prefer under natural circumstances. The temperature effect may be absent for the heat production in neonates due to small body volume, large body surface area-ratio, resulting in a 5% higher heat loss for neonates than in other size classes i.e. heat production from swimming muscles is 80% as reported for most fishes rather than 75% reported for endothermic fishes (Webb 1975). The difference may also account for other metabolic activities in the shark not estimated in this study. Adding the difference (22-64%) to the model (scaling coefficient *a*) would account for the total routine metabolic rate for neonates body mass 23-25 kg.

Although routine metabolic rate is not the same as basal metabolic rate, for a ram-ventilating fish routine metabolic rate must be the closest metabolic activity to rest i.e. basal metabolic rate. The scaling exponent in the great white shark (b = -0.28, fig. 14) is close to that reported in Schmidt-Nielsen (1984) for mammals (b = -0.25) or birds and bats (b = -0.27). It is also relatively close to Pacific bluefin tuna heat production (b = -0.39) reported in Kitagawa *et al.* (2006). The metabolic rate in the great white shark is close to flying endothermic animals (birds and bats) and to metabolic rate for mitochondria rich organs (b = -0.29) according to Schmidt-Nielsen (1984). This would indicate that mitochondria in the muscles of the shark are driving the heat production as have been suggested by Carey (1982).

Semmens *et al.* (2013) and Carey *et al.* (1982) present conflicting metabolic rates in terms of oxygen consumption. In Semmens *et al.* (2013) the metabolic rate is several times higher than in Carey *et al.* (1982) and this is based on that the swimming speed reported in Carey *et al.* (1982) was 3.2 km/h for a 4.6 total length great white shark. However Semmens *et al.* (2013) showed the sustained swimming speed to be much higher for adults. Furthermore the routine metabolic rate for neonate great white sharks (Ezcurra *et al.* 2012) was used to extrapolate the routine metabolic rate for an adult great white shark by combining the metabolic rate from neonate mako shark and observed swimming speed in adult great white sharks. By doing this three potential errors was done: 1) The mass specific metabolic rate is lower in larger sized animals throughout the animal kingdom, 2) another species was used to extrapolate the metabolic rate 3), the observed swimming speed in Carey *et al.* (1982) was 3.2 km/h however the sharks was reported to move southwest and thus likely against the Gulf Stream having an opposite speed of 5.4-6.48 km/h (Worthington 1954) implying the total effort in swimming speed produced by the 4.6 total length great white shark was likely observed swimming speed plus the Gulf Stream in opposite direction. The actual swimming speed without current would equal 8.6-9.7 km/h, close to the reported swimming speed in Semmens *et al.* (2013) and in this study (fig. 14) for adults. This means the metabolic measurements in Carey *et al.* (1982) are still valid (Table 2) and estimated routine metabolic rate in Semmens *et al.* (2013) is wrong.

Figure 14
Mass specific oxygen consumption mg O$_2$/kg h^{-1} (n = 16)
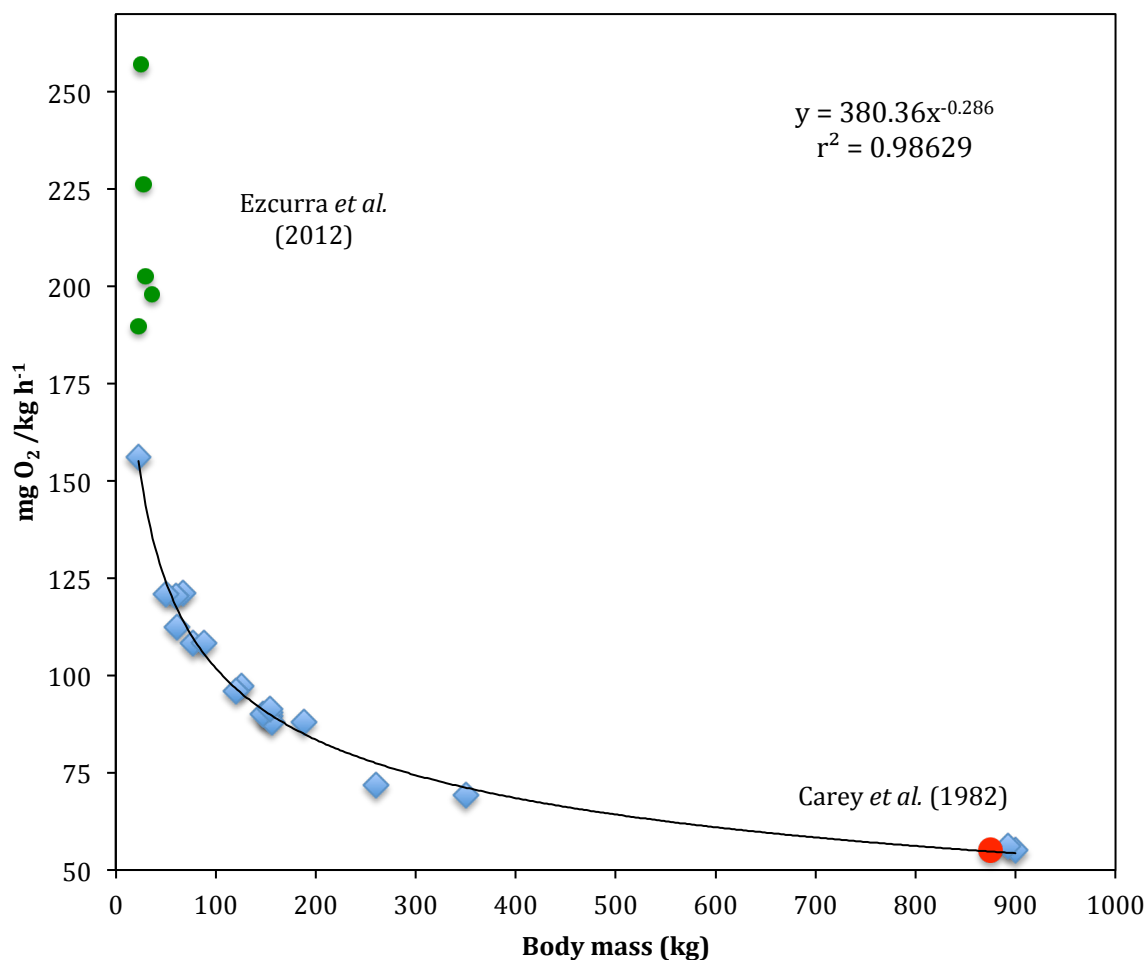

Figure 14: The routine metabolic rate (RMR) is the highest reported for any fish and fits close to the values (green spots, n = 5) from great white sharks held in captivity (Ezcurra *et al.* 2012). Those reported values and the estimated value from Carey *et al.* (1982) for a 4.6 total length great white shark (red, n = 1) are plotted with blue spots from this study.

4.4 Stomach volume and energy requirement

Daily energy requirements

The adult great white shark has the daily energetic requirement equivalent to that of two adult humans 2,400 kcal/day (Cole 2006). The estimate is comparable with Carey *et al.* (1982) being 0.2 kcal/kg h^{-1} which equals 4.8 kcal/kg per day. Without knowing the mass from the great white shark measured in the field this figure was extrapolated by Carey *et al.* (1982) using a body mass of 943 kg from a similar sized great white shark resulting in 4,526 kcal per day.

The daily caloric need in the great white shark was estimated in this study (fig. 16) using an allometric relationship from sustained swimming speed and body mass. The daily caloric need for an adult great white shark (PCL 3.63 m, 900 kg) is 4,871 kcal/day, which is over 30 times lower than another rivalling apex predator, the killer whale *Orcinus orca*. In an adult female killer whale

Orcinus orca (BM 3,338 kg) the energy requirement is 153,127 kcal/day (Noren 2011). The mass specific metabolic rate is much lower for the great white shark 5.4 kcal/kg day^{-1} compared to the adult female killer whale, being 45.9 kcal/kg day^{-1}. The killer whale has 8.5 times higher mass specific energy requirement. In fact the adult great white shark has the same energy requirement per day as two humans and a sub-adult great white shark have a similar energy requirement as one human. It is likely the higher energy requirement in a killer whale may have two explanations. The body temperature is higher of approximately 37°C while the warmest parts of the great white shark is 26°C or lower. Furthermore not all of the great white shark is heated in the same manner as the red muscles and secondly the brain of the killer whale is much larger, which is an organ of high energy expenditure. The metabolic scaling rate in killer whales is thus higher and different (b = 0.75, P = 0.0002) while bats and birds (b = 0.72, P = 0.3) have the same metabolic scaling rate as great white sharks (b = 0.71) probably because the latter show more of regional endothermy than well-isolated marine mammals.

The energy requirement estimated in this study do not include specific dynamic action (SDA) which in tunas is 35%, nor did estimates include energy requirements for growth or reproduction and somatic maintenance from other organs than the propulsion muscles. Visceral organs probably require a majority of the somatic energy requirement together with the heart, the central nervous system including brain while the rest of the energy is required by the skeletal muscles although the skeletal muscles may represent half the body mass (Schmidt-Nielsen 1984). The mass specific metabolic rate of the great white shark organs is unknown. The measurements from neonate great white sharks held in captivity (fig. 14) gives an indication of 22-64% difference to estimates for swimming muscles in this study using sustained swimming speed and oxygen consumption in similar sized neonates. This difference may be the residual energy requirement for other organs not accounted for except the specific dynamic action. The neonates were all measured for routine metabolic rate with no food in their stomachs that excludes SDA (Ezcurra *et al.* 2012).

By dividing the estimated energy requirement by the energy content in prey species, it is possible to estimate how well different prey fits to the energetic demand by the predator, assuming that the digestive efficiency is 100%. In the female killer whale (3,338 kg), 68 kg Chinook salmons *Oncorhynchus tshawytscha* is required per day to sustain the energetic demands (Osborne 1999, Noren 2011). For the adult great white shark (900 kg) having dissimilar energy requirements it would be 9 kg salmons per day i.e. 2 salmons (BM 4.5 kg containing 9,990 kcal each). The mass of the two salmons would be 1% of the body mass of the great white shark while for the killer whale the 68 kg salmons would be 2% of the body mass, this is within the anticipated prey consumption per days which usually varies between 1-3% in various predatory species (Secor 2008). Furthermore, the trophic level of the killer whale (Pauly *et al.* 1998) corresponds (trophic level 4.5) to that of the great white shark (Cortés 1999) indicating that those apex predators predate on similar prey species. This has also been well documented in terms of predation on pinnipeds and odontocetes for great white sharks and killer whales (Grandi *et al.* 2012, Coscarella *et al.* 2015, Long & Jones 1996, Long *et al.* 1996). The mass specific difference in energy requirement of those two apex predators inhabiting the same trophic level may e.g. differentiate in reproductive strategies. The great white sharks gives birth to 12 young (Compango 2001) while the killer whale only gives birth to one young (Asper *et al.* 1988). The lifespan is similar between those two apex predators being 59 years for killer whales (Amano *et al.* 2011) and 44 years great white sharks (Natanson & Skomal 2015, Winter & Cliff 1999) however the birth rate per year in the great white shark is unknown.

The body mass of a Cape fur seal is 4.5-360 kg (Fallows *et al*. 2012) and contains 40% blubber and 27% muscles of body mass (Davidsson & Cliff 2014). Whale blubber contains 6,667 kcal/kg (Carey *et al*. 1982) being 3 times more energetically beneficial than Chinook salmon. A 55 kg Cape fur seal would then at least contain 206,000 kcal and last 1.5 months for a 900 kg great white shark. The northern elephant seal have a blubber proportion of 48% of body mass (Kretzmann *et al*. 1993) and the grey seal 46% blubber proportion to body mass (Hall & McConnell 2007) and would therefore be suitable prey species. Blubber rich prey species plays a vital role for the adult great white sharks to sustain the daily energy requirements but also probably even more so for growth and reproduction. Furthermore, this suggests that the great white shark is an active predator when not aggregating around pinniped colonies where blubber rich prey occurs. Oceanic prey such as tunas and dolphins may be of equal importance (Table 3).

A readily citied example extrapolating the energetic requirement of the great white shark use 30 kg whale blubber (Carey *et al*. 1982, Semmens *et al*. 2013) estimated to contain 200,000 kcal. If a 900 kg great white shark were to eat 30 kg whale blubber it would sustain the energetic need for 1.5 months according to the results of the present study and Carey *et al*. (1982), the same as for a 55 kg Cape fur seal (Table 3). This means that the energy requirement is several times lower than previously proposed in Semmens *et al*. (2013). Carey *et al*. (1982) proposed 200,000 Kcal (swimming speed 3.2 km/h) would last 44.1 days for a 943 kg great white shark. Semmens *et al*. (2013) proposed the same shark would last 11.6 days adding a higher mean swimming speed to the shark of 10.48 km/h and adding a combination of neonate metabolic rate from great white sharks and mako shark to the 943 kg great white shark described by Carey *et al*. (1982). However the estimate in Semmens *et al*. (2013) were based on neonate great white shark mass specific oxygen consumption (Ezcurra *et al*. 2012) and the mass specific oxygen consumption in a neonate (3.9 kg) mako shark (Graham 1990). The mass specific metabolic rate for neonates is naturally higher (Schmidt-Nielsen 1997). The Gulf Stream may also have influenced the great white sharks swimming speed in Carey *et al*. (1982) as it was observed moving southwest during July indicating a north-eastward current between 5.4-6.48 km/h (Worthington 1954). Adding this reverse water friction, the actual speed of the shark would be 8.6-9.7 km/h, which is similar sustained swimming speed measured by Semmens *et al*. (2013) and calculated in this study for adults (mean 9.3 km/h), figure (15).

Metabolic rates may be used to explain population growth rates and estimate recovery rates from overfishing (Dowd *et al*. 2006). The great white shark is a cryptic species in terms of population size, due to high migration rate (Cliff *et al*. 1996), the routine metabolic rate may be a more accessible data to modulate the population growth rate in the great white shark for future studies due to the less accessible oceanic phase in the great white sharks life history (Weng *et al*. 2007).

Figure 15
Maximum stomach volume (*n* = 5)

Figure 15 shows a scatter plot with fitted power curve. The y-axis is labeled "Stomach volume (l)" ranging from 1 to 161, and the x-axis is labeled "Body mass (kg)" ranging from 60 to 970. The equation $y = 42.926x^{1.1662}$ and $r^2 = 0.95931$ are displayed.
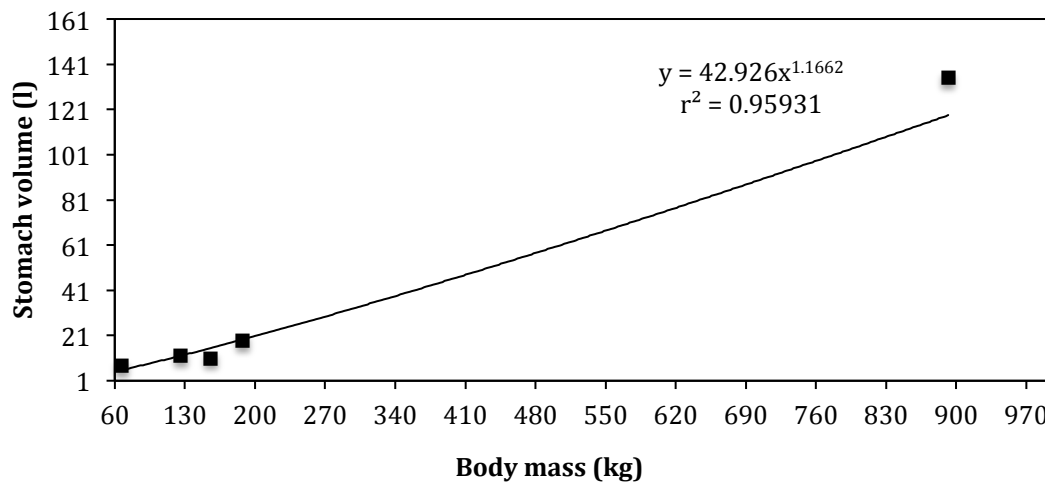
Figure 15: The maximum stomach volume in relation to body mass show an isometric growth in the great white shark.

Optimal prey based on stomach volume and energy requirement

Measuring the maximum stomach volume, the actual tissue mass a great white shark is able to ingest may be estimated and in more detailed studies the energy required to heat, digest and assimilate the stomach contents. The largest great white shark (892 kg) for in which the stomach volume was measured in this study had a stomach volume >135 litres, translating to a digestion of prey item reaching at least 120.15 kg in mammalian blubber. Adipose tissue density for the elephant seals genus *Mirounga* is 0.89 g/cm^3 (Schwarz *et al.* 2015).

Observations of fully consumed blue sharks *Prionace glauca* and dolphins (family Delphinidae) and even pinnipeds have been documented (Fergusson 1996, Cliff *et al.* 1989, Klimley 1985, Postel 1958), confirming the accuracy of the maximum stomach volume model in this study (Table 2, fig. 15). Although the sample size is small (*n* = 5), the model could be used for first hand energetic calculations (Table 3); this is of particular interest when investigation transoceanic migrations patterns displayed by great white sharks (Bonfil *et al.* 2005) or investigating how far the great white shark may swim on different stomach contents.

Moreover knowing the daily energy requirement for different life stages in the great white shark, optimal prey item may be elucidated (Table 3) and indicate habitat use. In a neonate great white shark the stomach volume is estimated to 1.7 litres. If this shark would be able to eat from a whale carcass it could sustain itself on 1 kg whale blubber for 19 days. Neonates have been observed feeding on a whale carcass in Algoa Bay, South Africa (Dicken 2008). The most accessible prey species are probably smaller fish species and squids (Hussey *et al.* 2012, Smale & Cliff 2012) and thus the most optimal prey, a 1 kg of herring or pilchard (or equal) would sustain a 23 kg neonate for approximately a week. The 1 kg squid would only sustained one third of a day and with limited stomach volume this would not be a fitting prey item in neonates (Table 3). Whale blubber stands out as the best food item for all great white sharks and is probably important for growth and reproduction due to the low energy cost to effort of consuming this food item. In Fallows *et al.* (2013) whale carcasses was suggested to be of significant importance to adult great white sharks.

Figure 16
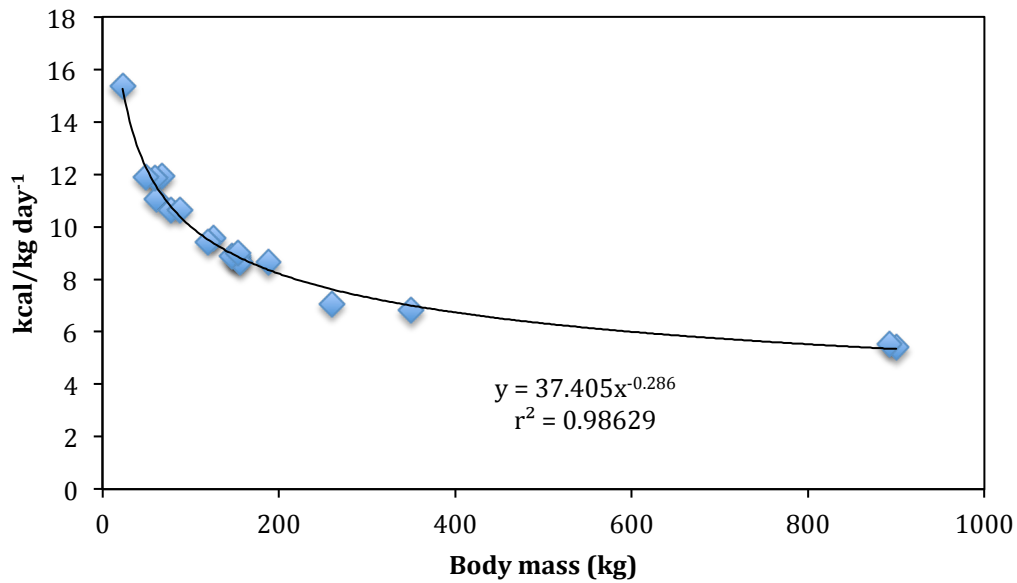**Mass specific daily energy requirement (*n* = 16)**

Figure 16: Showing the kilocalories (kcal) needed per kilogram (kg) body mass per day for sustained swimming. Mass specific metabolism decrease with increase of body size (*b* = -0.28). See Table 2 for details of results.

Figure 17
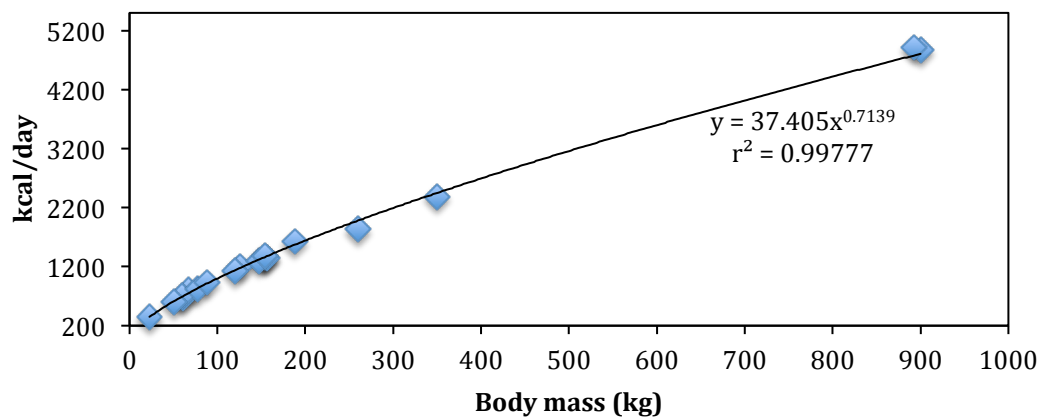**Daily energy requirement (*n* = 16)**

Figure 17: Showing the total kcal/day in body mass where *b* = 0.71. The result indicates that the great white shark has similar metabolic rate as mammals and birds. See Table 2 for details.

In juveniles the stomach volume have increased to 12 litres and according to Table (3) the most optimal prey would be a 10 kg Cape fur seal which would sustained the shark for one month followed by a 10 kg skipjack tuna which would sustain the energy requirements for almost two weeks (Table 3). Most of the prey items found in stomach contents from juveniles are pelagic teleosts suggesting the tuna is the most important prey but if the occasion arise a juvenile Cape fur seal would be the most optimal prey. This may be why those great white sharks are observed as far west in South Africa as False Bay (Kock *et al.* 2013). Juveniles and sub-adults have similar mass

specific heat production of 8°C/kg h^{-1} (fig. 9) indicating juveniles have capacity to inhabit similar temperatures as sub-adults. However the presence of adults and sub-adults in the Western Cape near seal colonies likely pose a risk for juveniles resulting in a spatial size-based segregation.

A sub-adult would be optimally sustained on a 30 kg Cape fur seal (Table 3). This prey would give the shark 1.5 months of sustained swimming. The adult great white shark would be sustained on the same prey for almost a month but the most optimal prey for adults is surprisingly a 100 kg common dolphin followed by a 55 kg the Cape fur seal (Table 3). If however the adult great white shark would consume a Cape fur seal in the size of 100 kg this is the optimal prey. When comparing skipjack tuna and common dolphin (Table 3), the dolphin have higher energy content and is apparently twice as calorie-rich as the tuna. Considering the common dolphin is up to four times slower in burst speed than some tuna species (Rohr *et al.* 2013, Sambilay 1990) it is likely dolphins is the preferred prey prior to tunas during the oceanic phase. Dolphins have also been reported to consist a large part (26% of the diet) in Mediterranean great white sharks; an area where pinnipeds do not exists any longer (De Maddalena & Heim 2012). Taking the data from the Mediterranean in consideration and results from this study (Table 3), suggests dolphins may be an important prey during the oceanic phase for the adult great white shark. Oceanic aggregations of great white sharks as seen in the Pacific Ocean (Weng *et al.* 2007) may possibly correlate to occurrence of dolphins. Ranking prey by their energy contents versus energy cost (burst speeds) for the adult great white shark, the following prey preference could be expected; 1) whale blubber 2) pinnipeds 3) dolphins 4) tunas (Table 3).

The distance a great white shark may swim before it needs to feed again, assuming 100% assimilation efficiency, can be estimated using (Schmidt-Nielson 1972) to calculate kcal/km. In the case of a ca. 900 kg great white shark (4,871 kcal/day), this would be 203 kcal/h with swim speed approximately 10 km/h equal to 20 kcal/km. Knowing the full stomach volume to contain 120 kg whale blubber equal (800,040 kcal), a great white shark would be able to swim the circumference the Earth (40,000 km) during several years on a full stomach whale blubber. It is however more likely the energy surplus is used for reproduction and growth rather than a turnover in swimming distances. In great white sharks that are mature and have a limited growth it is especially likely the energy is used for reproduction. In fact whale blubber may be significant for great white shark reproduction and migration (Fallows *et al.* 2013). The importance of whale blubber for the great white shark is well-illustrated by events, e.g. where a Brydes´s whale *Balaenoptera edeni* carcass (11 m) observed to be partly consumed by up to 40 great white sharks during a 5 hours observation time, in False Bay, South Africa (Fallows *et al.* 2013).

Based on migrating swimming speeds with sinuous swimming paths and current obstruction included (Bonfil *et al.* 2005, Weng *et al.* 2007) it is reasonable to estimate the swimming speed to 5 km/h and the migration distance to 20,000 km equalling a distance between South Africa and Australia and back again for twice the time presented in Bonfil *et al.* (2005). The great white shark has been documented to cover the distance between South Africa and Australia (11,100 km) in 99 days at a mean swimming speed of 4.7 km/h (Bonfil *et al.* 2005). Using the total length (TL 3.8 m) for the great white shark described in Bonfil *et al.* (2005), the amount of whale blubber needed may be extrapolated. By calculating precaudal length and body mass (Cliff *et al.* 1996), calculation indicates a size in precaudal length of 2.97 m and body mass to 408.6 kg. The maximum stomach volume is calculated to 47.6 litres using the model in figure (15) and the sustained swimming speed is 8.6 km/h (fig. 15). The great white shark described in Bonfil *et al.* (2005) had a daily energy requirement of 2,736 kcal/day (fig. 17, Table 2) or in total 114 kcal/h resulting in 13 kcal/km.

Swimming 11,000 km equals 145,813 kcal, thus it had to eat 14 Chinook salmons or 21 kg whale blubber during its one-way transoceanic migration, using the energetic need and swimming speed described in this study (Table 2). Since we know the travel time for this one-way transoceanic migration we can also calculate how many kilos that is ingested per day. In the case of blubber it would need to eat 0.22 kg daily or 0.14 Chinook salmons (body mass 4.5 kg) per day equalling 630 grams/day of salmons or one salmon every 4.5/days. Both food items fit into the stomach (Table 2). A full stomach of blubber (47.6 litres) would last 24,410 km or 115 days that is from Africa to Australia and back again. That is very close to the reported traveling time of 99 days (Bonfil *et al.* 2005).

In conclusion, the great white shark that crossed the Indian Ocean did not have to eat at all during the migration, if a large high calorie meal was consumed before onset of migration. Otherwise it would need to eat a larger fish once a week during the transoceanic migration from South Africa to Australia based on the estimated swimming speed being 8.6 km/h (fig. 13, Table 2) instead of 4.7 km/h in Bonfil *et al.* (2005) due to probable underestimation of swimming speed (Weng *et al.* 2007) as a result of ocean currents, drift dives and sinus swimming.

In Del Reye *et al.* (2013) the buoyancy of migrating great white sharks showed a gradual decrease during travel, this might indicate that those sharks prepare for migration by eating large quantities of lipid rich food before travel and lose this as it is digested. Oceanic predation has been documented using stable isotope analysis and to occur at a decreased rate compared to predation in costal areas (Carlisle *et al.* 2012). It is therefore likely that great white sharks engaged in transoceanic migrations still have a predatory behaviour, but with a lower success rate than what is commonly observed during the neritic phase, e.g. where pinnipeds congregate in small geographic areas and other prey species. Occasional squid predation may be common (Smale & Cliff 2012) as a result of drift diving through the water column in search of larger prey species. Dolphins and tunas (Table 3) together with whale carcasses (Fallows *et al.* 2013) are probably the most important food available during the oceanic phase (Table 3 – this study, Carlisle *et al.* 2012, Fallows *et al.* 2013)

Table 3: Example of prey species showing body mass with calculated kcal. Using four different individuals from each size class (Table 1) and their body mass (kg), estimated energetic requirement per day (kcal/day, fig. 17, Table 2) and their respectively stomach volume (l) (fig. 15, Table 2). The energy content (kcal prey) was estimated from the references in the far right column. Rows with strokes indicate prey do not fit in maximum stomach volume.

			Neonate	Juvenile	Sub-adult	Adult	
	Body mass (kg)		23	126	350	900	
	kcal/day		353	1,206	2,382	4,871	
	Stomach volume (l)		1.7	12.1	39.8	119.7	
Prey species	**Mass (kg)**	**kcal prey**	**Days**	**Days**	**Days**	**Days**	**Reference**
Cape fur seal	55	206,067	-	-	-	42	Davidsson & Cliff 2014
Cape fur seal	30	112,400	-	-	47	23	Davidsson & Cliff 2014
Cape fur seal	10	37,467	-	31	16	8	Davidsson & Cliff 2014
Common dolphin	100	305,200	-	-	-	63	Davidsson & Cliff 2014
Common dolphin	50	152,600	-	-	-	31	Davidsson & Cliff 2014
Whale blubber	1	6,666.7	19	6	3	1	Carey *et al.* 1982
Whale blubber	30	200,001	-	-	84	41	Carey *et al.* 1982
Whale blubber	40	266,668	-	-	112	55	Carey *et al.* 1982
Whale blubber	100	666,670	-	-	-	137	Carey *et al.* 1982
Skipjack tuna	1	1,500	4	1	1	0	Kitchell *et al.* 1977
Skipjack tuna	5	7,500	-	6	3	2	Kitchell *et al.* 1977
Skipjack tuna	10	15,000	-	12	6	3	Kitchell *et al.* 1977
Skipjack tuna	50	75,000	-	-	-	15	Kitchell *et al.* 1977
Skipjack tuna	100	150,000	-	-	-	31	Kitchell *et al.* 1977
Mackerel	1	1,888.1	5	2	1	0	Spitz *et al.* 2010
Catshark	1	1,529.6	4	1	1	0	Spitz *et al.* 2010
Skate	1	1,362.3	4	1	1	0	Spitz *et al.* 2010
Herring	1	2,437.9	7	2	1	1	Spitz *et al.* 2010
Pilchard	1	2,079.3	6	2	1	0	Spitz *et al.* 2010
Silver seabream	4.5	2,246.6	-	2	1	0	Semmens *et al.* 2013
Squid	1	114.7	0.3	0.1	0	0	Spitz *et al.* 2010

5. ACKNOWLEDGEMENTS

6. REFERENCES

Alexander R MCN. (1959). The densities of Cyprinidae. Journal of Experimental Biology. Vol. 36: Pp. 333-340.

Alexander, R.L. (1998). Blood supply to the eyes and brain of lamniform sharks (Lamniformes). Journal of Zoology. London. Vol. 245, 363–369.

Amano M., Yamada T.K., Brownwell R.L, Uni Y. (2011). Age determination and reproductive traits of killer whales entrapped in ice off Aidomari, Hokkaido, Japan. Journal of Mammalogy, Volume 92(2): Pp. 275–282.

Andreotti, S., von der Heyden, S., Henriques, R., Rutzen, M., Meÿer, M., Oosthuizen, H. and Matthee, C. A. (2016), New insights into the evolutionary history of white sharks, *Carcharodon carcharias*. Journal of Biogeography, 43: 328–339. doi:10.1111/jbi.12641

Asper E.D., Young W.G., Walsh M.T. (1988). Observations on the birth and development of a captive-born Killer whale *Orcinus orca*. International Zoo Yearbook, 27: Pp. 295–304.

Bass AJ. (1973). Analysis and description of variation in the proportional dimensions of Schyliorhind, Carcarhind and Spyrhind sharks. Investigational report No. 32, Oceanographic Research Institute. South African Association for Marine Biological Research. Pp. 28.

Bass AJ, D'Aubrey JD & Kistnasamy N. (1975). Sharks ofthe east coast of Southern Africa. IV. The families Odontasipididae, Scapanorhynchidae, Isuridae, Cetorhinidae, Alopiidae, Orectolobidae and Rhiniodontidae. Bulletin South African Association for Marine Biological Research 39. 22–26.

Bernal D, Carlson JK, Goldman KJ, Lowe CG. (2012). Energetics, Metabolism, and Endothermy in Sharks and Rays. In: Carrier JC, Musick JA, Heithaus MR (Eds.). Biology of Sharks and their Relatives, Edition 2. CRC Press, Boca Raton, Florida: 211-238.

Bernal D, Donley JM, Shadwick RE, Syme DA. (2005). Mammal-like muscles power swimming in a cold-water shark. Nature, Volume 437: Pp. 1349-1352.

Bernal D, Sepulveda C, Mathieu-Costello O, Graham JB. (2003). Comparative studies of high performance swimming in sharks I. Red muscle morphometrics, vascularization and ultrastructure. The Journal of Experimental Biology 206, Pp. 2831-2843.

Bernal S, Dickson KA, Shadwick RE, Graham JB. (2001). Review: Analysis of the evolutionary convergence for high performance swimming in lamnid sharks and tunas. Comparative Biochemistry and Physiology Part A: Molecular & Integrative Physiology Volume 129, Issues 2–3, Pp. 695–726.

Bertalanffy L. von (1960). Principles and theory of growth, pp 137-259. In: W. W. Wowinski (ed.). Fundamental aspects of normal and malignant growth. Elseviers Publishing Company, Amsterdam.

Blamey LK, Shannon LJ, Bolton JJ, Crawford RJM, Dufois F, Evers-King H, Griffiths CL, Hutchings L, Jarre A, Rouault M, Watermeyer KE, Winker H. (2015). Ecosystem change in the southern Benguela and the underlying processes. Journal of Marine Systems, 144: Pp. 9–29.

Block BA & Carey FG. (1985). Warm brain and eye temperatures in sharks. Journal of Comparative Physiology B:

Biochemical, Systemic, and Environmental Physiology, 156 (2): Pp. 229-236.

Bonfil R, Mey M, Scholl MC, Johnson R, O'Brien S, Ossthuizen H, Swanson S, Kotze D, Paterson M. (2005). Transoceanic migration, spatial dynamics, and population linkages of white sharks. Science, Volume 310: Pp. 100-103.

Bonfil R, Francis MP, Duffy C, Manning MJ, O'Brien S. (2010). Large-scale tropical movements and diving behavior of white sharks *Carcharodon carcharias* tagged off New Zealand. Aquatic Biology, Volume 8, no. 2: Pp. 115–123.

Boustany AM, Davis SF, Pyle P, Anderson SD, Le Boeuf BJ, Block BA. (2002). Expanded niche for white sharks. Nature, Volume 415: Pp. 35–36.

Brill RW, Dewar H, Graham JB. (1994). Basic concepts relevant to heat transfer in fishes, and their use in measuring the physiological thermoregulatory abilities of tunas. Environmental Biology of Fishes, Volume 40, Issue 2: Pp. 109-124.

Bruce BD, & Bradford RW. (2012). Habitat use and spatial dynamics of juvenile white sharks, *Carcharodon carcharias*, in Eastern Australia. In: Domeier ML. (Ed.) Global Perspectives on the Biology and Life History of the Great White Shark. CRC Press: Chapter 17: Pp. 225-253.

Burne RH. (1923). Some peculiarities of the blood vascular system of the porbeagle shark (*Lamna comubica*). Philosophical Transactions of the Royal Society of London. 212B: Pp. 1923-1924.

Carey FG. (1982). Warm Fish. In: Taylor CR, Johansen K, Bolis L. (Eds.). A Companion to Animal Physiology. Cambridge University Press, Chapter 16: Pp. 216-233.

Carey F.G. & Teal J.M. (1969). Mako and porbeagle: Warm-bodied sharks. Comparative Biochemistry and Physiology. Volume 28, Pp. 199-204.

Carey FG, Teal JM, Kanwisher JW, Lawson KD, Beckett JS. (1971). Warm-Bodied Fish. American Zoologist, Volume 11, No. 1. Pp. 135-143.

Carey FG & Teal, JM. (1969). Mako and porbeagle: Warm-bodied sharks. Comparative Biochemistry and Physiology 28: Pp. 199–204.

Carey FG, Casey JG, Pratt HL, Urquhart D, McCosker JE. (1985). Temperature, heat production and heat exchange in lamnid Sharks. In: Sibley, G. (Ed.). Biology of the White Shark, a Symposium. Los Angeles: Southern California Academy of Sciences, Memoirs of the Southern California Academy of Sciences, Volume 9: Pp. 92-108.

Carey FG, Kanwisher JW, Brazier O, Gabrielson G, Casey JG, Pratt, HL Jr. (1982). Temperature and activities of a white shark, *Carcharodon carcharias*. Copeia (2): Pp. 254–260.

Carey FG, Teal JM, Kanwisher JW. (1981). The visceral temperatures of mackerel sharks (Lamnidae). Physiological Zoology, Volume 54, No. 3: Pp. 334–344.

Carlisle AB, Goldman KJ, Litvin SY, Madigan DJ, Bigman JS, Swithenbank AM, Kline TC, Block BA. (2015). Stable isotope analysis of vertebrae reveals ontogenetic changes in habitat in an endothermic pelagic shark. Proceedings of the Royal Society of London B: Biological Sciences, 282 (1799): 20141446 DOI: 10.1098/rspb.2014.1446.

Carlisle AB, Kim SL, Semmens BX, Madigan DJ, Jorgensen SJ, Perle CR, Anderson SD, Chapple TK, Kanive PE, Block BA. (2012). Using Stable Isotope Analysis to Understand the Migration and Trophic Ecology of Northeastern Pacific White Sharks (*Carcharodon carcharias*). PLoS ONE 7(2): e30492. doi:10.1371/journal.pone.0030492

Carlisle AB, Kim SL, Semmens BX, Madigan DJ, Jorgensen SJ. (2012). Using stable isotope analysis to understand the migration and trophic ecology of northeastern pacific white sharks (*Carcharodon carcharias*). PLoS ONE 7(2): e30492. doi:10.1371/journal.pone.0030492

Carlson JK, Goldman KJ, Lowe CG. (2004). Metabolism, Energetic Demand, and Endothermy. In: Carrier JC, Musick JA, Heithaus MR (Eds.). Biology of Sharks and their Relatives. Chapter 7: Pp. 203-224.

Casey, J.G. & Pratt, H.L. (1985). Distribution of the white shark, *Carcharodon carcharias*, in the western North Atlantic. In: Sibley, G. (Ed.). Biology of the White Shark, a Symposium. Los Angeles: Southern California Academy of Sciences, Memoirs of the Southern California Academy of Sciences, Volume 9: Pp. 2-14.

Cheverud JM. (1982). Relationships among ontogenetic, static, and evolutionary allometry. American Journal of Physical Anthropology Volume 59, Issue 2, Pp. 139–149.

Cliff G & Dudley SFJ. (2011). Reducing the environmental impact of shark-control programs: a case study from KwaZulu-

Natal, South Africa. Marine and Freshwater Research, 62 (6): Pp. 700-709.

Cliff G, Dudley SFJ, Davis B. (1988). Sharks caught in the protective gill nets off Natal, South Africa. 1. The sandbar shark *Carcharhinus plumbeus* (Nardo). South African Journal of Marine Science, 7 (1): Pp. 255-265 DOI: 10.2989/025776188784379035

Cliff G, Dudley SFJ, Davis B. (1989). Sharks caught in the protective gill nets off Natal, South Africa. 2. The great white shark *Carcharodon carcharias*. South African Journal of Marine Science, 8 (1): Pp. 131-144.

Cliff G, Dudley SFJ, Jury MR. (1996). Catches of white sharks in KwaZulu-Natal, South Africa and environmental influences. In: Klimley, A.P. & Ainley, D. (Eds.) Great White Sharks. The biology of *Carcharodon carcharias*: Pp. 351- 362.

Cole J. (2006). Cannibalism, prehistoric cannibalism, nutritional values for cannibalism. Dissertation. Faculty of law, arts and social sciences. University of Southampton. Pp. 1-97.

Compagno LJV. (1990). Relationships of the megamouth shark, *Megachasma pelagios* (Lamniformes: Megachasmidae), with comments on its feeding habits. NOAA Technical Report, NMFS 90: Pp. 357-379.

Compagno LJV. (2001). Sharks of the world. An annotated and illustrated catalogue of shark species known to date. Volume 2. Bullhead, mackerel and carpet sharks (Heterodontiformes, Lamniformes and Orectolobiformes). FAO species catalogue for fishery purposes No. 1, Vol. 2. Rome: FAO. 269 Pp.

Cortés E. (1999). Standardized diet compositions and trophic levels of sharks. ICES Journal of Marine Science, 56: Pp. 707–717.

Coscarella MA, Bellazzi G, Gaffet ML, Berzano M, Degrati M. (2015). Short Note: Technique Used by Killer Whales (*Orcinus orca*) When Hunting for Dolphins in Patagonia, Argentina. Aquatic Mammals 2015, 41(2), Pp. 192-197, DOI 10.1578/AM.41.2.2015.192.

Costa DP, Robinson PW, Arnould JPY, Harrison A-L, Simmons SE, Hassrick JL, Hoskins AJ, Kirkman SP, Oosthuizen H, Villegas-Amtmann S, Crocker DE. (2010). Accuracy of ARGOS Locations of Pinnipeds at-Sea Estimated Using Fastloc GPS. PLoS ONE 5(1): e8677. doi:10.1371/journal.pone.0008677

Coughlin D.J. & Rome L.C. (1996). The roles of pink and red muscle in powering steady swimming in scup, *Stenotomus chrysops*. Integrative and Comparative Biology. Volume 36, Issue 6: Pp. 666-677.

Curtis TH, McCandless CT, Carlson JK, Skomal GB, Kohler NE, et al. (2014). Seasonal distribution and historic trends in abundance of white sharks, *Carcharodon carcharias*, in the western North Atlantic Ocean. PLoS ONE 9(6): e99240. doi:10.1371/journal.pone.0099240

Davidsson B. & Cliff G. (2014). Comparison of pinniped and cetacean prey tissue lipids with lipids of their elasmobranch predator. In vivo, International Journal of Experimental and Clinical Pathophysiology and Drug Research. 28: Pp. 223-228.

De Maddalena, A. & Zuffa, M. (2009). Historical and contemporary presence of the great white shark, *Carcharodon carcharias* (Linnaeus, 1758), along the Mediterranean coast of France. Bollettino del Museo civico di Storia Naturale di Venezia, 59: Pp. 81–94.

Del Raye G, Jorgensen SJ, Krumhansl K, Ezcurra JM. Block, BA. (2013). Travelling light: white sharks (*Carcharodon carcharias*) rely on body lipid stores to power ocean-basin scale migration. Proceedings of the Royal Society of London, Series B. 280 (1766): Pp. 1-9.

Dewar H, Graham JB, Brill RW. (1994). Studies of tropical tuna swimming performance in a large water tunnel II. Thermoregulation. Journal of Experimental Biology Volume, 192, issue 1 Pp. 33-44.

Dewar H, Domnier ML, Nasby-Lucas N. (2004). Insights into young of the year white shark, Carcharodon carcharias, behavior in the Southern California Bight. Environmental Biology of Fishes, 70: Pp. 133–143.

Dicken ML. (2008). First observations of young of the year and juvenile great white sharks (*Carcharodon carcharias*) scavenging from a whale carcass. Marine and Freshwater Research, 59 (7): Pp. 596-602 DOI: 10.1071/MF07223

Dicken ML. & Booth AJ. (2013). Surveys of white sharks (*Carcharodon carcharias*) off bathing beaches in Algoa Bay, South Africa. Marine and Freshwater Research, 64: Pp. 530–539.

Dicken ML, Smale MJ, Booth AJ. (2013). White sharks *Carcharodon carcharias* at Bird Island, Algoa Bay, South Africa. African Journal of Marine Science, 35:2: Pp. 175-182.

Dickson KA (1995). Unique adaptations of the metabolic biochemistry of tunas and billfishes for life in the pelagic environment. Environmental Biology of Fishes. Volume 42: Pp. 65-97.

Donley JM, Sepulveda CA, Konstantinidis P, Gemballa S, Shadwick RE. (2004). Convergent evolution in mechanical design of lamnid sharks and tunas. Nature, Volume 429, Pp. 61-65.

Dowd WW, Brill RW, Bushnell PG, Musick JA. (2006). Standard and routine metabolic rates of juvenile sandbar sharks (*Carcharhinus plumbeus*), including the effects of body mass and acute temperature change. Fishery Bulletin, Volume 104, Issue 3, Pp. 323-331.

Emery SH. (1985). Hematology and Cardiac Morphology in the Great White Shark, *Carcharodon carcharias*. In: Sibley, G. (Ed.). Biology of the White Shark, a Symposium. Los Angeles: Southern California Academy of Sciences, Memoirs of the Southern California Academy of Sciences, volume 9: Pp. 73-80.

Ezcurra JM, Lowe CG, Mollet HF, Ferry LA, O'Sullivan JB. (2012). Oxygen consumption rate of young-of-the-year white shark, *Carcharodon carcharias*, during transport to the Monterey Bay aquarium. In: Domeier, ML. (Ed.) Global Perspectives on the Biology and Life History of the Great White Shark. CRC Press: Chapter 2: Pp. 17-25.

Fallows C, Martin RA, Hammerschlag N. (2012). Comparisons between White Shark–Pinniped Interactions at Seal Island (South Africa) with Other Sites in California. In: Domeier, M. L. (Ed.) Global Perspectives on the Biology and Life History of the Great White Shark. CRC Press: Chapter 9: Pp. 105-120.

Fallows C, Gallagher AJ, Hammerschlag N (2013). White sharks (*Carcharodon carcharias*) scavenging on whales and its potential role in further shapingthe ecology of an apex predator. PLoS ONE 8(4): e60797. doi:10.1371/journal.pone.0060797

Fergusson IK. (1996). Distribution and autecology of the white shark in the Eastern North Atlantic Ocean and the Mediterranean Sea. In: Klimley AP. & Ainley D. (Eds.) Great White Sharks. The biology of *Carcharodon carcharias*: Chapter 30: Pp. 321-347.

Ferreira CA & Ferreira TP. (1996). Population dynamics of the white sharks in South Africa. In: Klimley AP & Ainley D. (Eds.) Great White Sharks. The biology of *Carcharodon carcharias*: Chapter 35: Pp. 381-391.

Fitzgibbon QP, Seymour RS, Ellis D, Buchanan J. (2006). The energetic consequence of specific dynamic action in southern bluefin tuna *Thunnus maccoyii*.The Journal of Experimental Biology. Pp. 290-298.

Francis MP, Duffy CAJ, Bonfil R, Manning MJ. (2012). The third dimension. Vertical habitat use by white sharks, *Carcharodon carcharias*, in New Zealand and in oceanic and tropical waters of the southwest Pacific Ocean. In: Domeier ML. (Ed.) Global Perspectives on the Biology and Life History of the Great White Shark. CRC Press: Chapter 22: Pp. 319-342.

Gallon SL, Sparling CE, Georges JY, Fedak MA, Biuw M, Thompson D. (2007). How fast does a seal swim? Variations in swimming behaviour under different foraging conditions. The Journal of Experimental Biology. Volume 210. Pp. 3285-3294.

Goldman KJ. (1997). Regulation of body temperature in the white shark, *Carcharodon carcharias*. Journal of Comparative Physiology B: Biochemical, Systemic, and Environmental Physiology, 167 (6): Pp. 423-429.

Goldman KJ, Anderson SD, McCosker JE, Kimley AP. (1996). Temperature, swimming depth, and movements of a white shark at the South Farallon Islands, California. In: Klimley, A.P. & Ainley, D. (Eds.) Great White Sharks. The biology of Carcharodon carcharias: Chapter 11: Pp. 111-120.

Gould SJ. (1966). Allometry and size in onotgeny and phylogeny. Biological Reviews, 41: Pp. 587–638. doi: 10.1111/j.1469-185X.1966.tb01624.x.

Graham JB, Dewar H, Lai NC, Lowell WR, Arce SM (1990). Aspects of shark swimming performance using a large water tunnel. Journal of Experimental Biology. Volume 51. Pp. 175-192.

Graham JB, Kohern FJ, Dickson KA. (1983). Distribution and relative proportions of red muscle in scombrid fishes: consequences of body size and relationships to locomotion and endothermy. Canadian Journal of Zoology, 61(9): Pp. 2087-2096, 10.1139/z83-274.

Grandi MF, Loizaga de Castro R, Crespo EA. (2012). Short communication: Killer whales attack on South American sea lion associated with a fishing vessel: predator and prey tactics. Latin American Journal of Aquatic Research. 40(4): Pp. 1072-

1076.

Gubili C, Bilgin R, Kalkan E, Karhan SU, Jones CS. Sims DW, Kabasakal H, Martin AP, Noble LR. (2010). Antipodean white sharks on a Mediterranean walkabout? Historical dispersal leads to genetic discontinuity and an endangered anomalous population. Proceedings of the Royal Society B. 278: Pp. 1679–1686.

Hall, A. J. and McConnell, B. J. (2007). Measuring changes in juvenile gray seal body composition. Marine Mammal Science, 23: Pp. 650–665.

Hammerschlag N, Martin RA, Fallows C. (2006). Effects of environmental conditions on predator–prey interactions between white sharks (*Carcharodon carcharias*) and Cape fur seals (*Arctocephalus pusillus pusillus*) at Seal Island, South Africa. Environmental Biology of Fishes. Volume 76, Issue 2, Pp. 341-350.

Hubbell G. (1996). Using tooth structure to determine the evolutionary history of the white shark. In: Klimley, AP & Ainley D. (Eds.) Great White Sharks. The biology of *Carcharodon carcharias*: Chapter 3: Pp. 9-18.

Hussey NE, McCann HM, Cliff G, Dudley SFJ, Winter SP, Fisk AT. (2012). Size-based analysis of diet and trophic position of the white shark, *Carcharodon carcharias*, in South African waters. In: Domeier ML. (Ed.) Global Perspectives on the Biology and Life History of the Great White Shark. CRC Press: Chapter 3: Pp. 27-49.

Huxley JS. (1924). Constant differential growth-ratios and their significance. Nature 114(2877):Pp. 895-896.

Huxley JS. & Tessier G. (1936). Terminology of relative growth. Nature 137: Pp. 780–781.

Kitagawa T, Kimura S, Nakata H, Yamada H. (2006). Thermal adaptation of Pacific bluefin tuna *Thunnus orientalis* to temperate waters. Fisheries Science, Volume 72: Pp. 149-156.

Kitchell JF, Magnuson JJ, Neil WH. (1977). Estimation of caloric content for fish biomass. Environmental Biology of Fishes, Volume 22: Pp. 185-188.

Kleiber M. (1932). Body size and metabolism. Hilgardia. Volume 6. Number 11: Pp. 316-353.

Klimley AP, Pyle P, Anderson SD. (1996). The Behavior of White Sharks and Their Pinniped Prey during Predatory Attacks. In: Klimley AP & Ainley D. (Eds.) Great White Sharks. The biology of *Carcharodon carcharias*: Chapter 16: Pp. 175-191.

Klimley AP. (1985). The Areal and Autoecology of the white shark, *Carcharodon carcharias*, off the West Coast of North America. In: Sibley G. (Ed.). Biology of the White Shark, a Symposium. Los Angeles: Southern California Academy of Sciences, Memoirs of the Southern California Academy of Sciences, Vol. 9: Pp. 15-40.

Kock A, O'Riain MJ, Mauff K, Mey¨er M, Kotze D, Griffiths C. (2013). Residency, Habitat Use and Sexual Segregation of White Sharks, *Carcharodon carcharias* in False Bay, South Africa. PLoS ONE 8(1): e55048. doi:10.1371/journal.pone.0055048

Kretzmann MB, Costa DP, Le Boeuf BJ. (1993). Maternal energy investment in elephant seal pups: evidence for sexual equality? The American Naturalist, Vol. 141, No 3: Pp. 466–480.

Lingham-Soliar T. (2005a). Caudal fin allometry in the white shark *Carcharodon carcharias*: implications for locomotory performance and ecology. Naturwissenschaften, 92: Pp. 231–236.

Lingham-Soliar, T. (2005b). Caudal fin in the white shark, *Carcharodon carcharias* (Lamnidae): A dynamic propeller for fast, efficient swimming. Journal of Morphology. Vol. 264: Pp. 233–252. doi: 10.1002/jmor.10328

Long, DJ. (1996). Records od White Shark-Bitten Leatherback Sea Turtles along the Central California Coast. In: Klimley AP & Ainley D. (Eds.) Great White Sharks. The biology of *Carcharodon carcharias*: Chapter 29: Pp. 317-319.

Long DJ. & Jones RE. (1996). White Shark Predation and scaveging on cetaceans in the Eastern North Pacific Ocean. In: Klimley AP & Ainley D. (Eds.) Great White Sharks. The biology of *Carcharodon carcharias*: Chapter 27: Pp. 293-307.

Lowe CG & Goldman KJ. (2001). Thermal and bioenergetics of elasmobranchs: Bridging the gap. Environmental Biology of Fishes. 60: Pp. 251–266.

Martin RA. (2004). Northerly Distribution of White Sharks, *Carcharodon carcharias*, in the Eastern Pacific and Relation to ENSO Events. Marine Fisheries Review. 66:1, Pp. 16-19.

Martin RA, & Hammerschlag N. (2012). Marine predator-prey contests: Ambush and speed versus vigilanceand agility. Marine Biology Research; 8: Pp. 90-94.

Martin RA, Hammerschlag N, Collier RS, Fallows C. (2005). Predatory behavior of white sharks (*Carcharodon carcharias*) at

Seal Island, South Africa. Journal of Marine Biology Association U.K. Vol. 85: Pp. 1121–1135.

McCosker JE. (1987). The white shark, *Carcharodon carcharias*, has a warm stomach. Copeia 1: Pp. 195–197.

Mollet HF & Cailliet GM (1996). Using allometry to predict body mass from linear measurements of the white shark. In: Klimley AP & Ainley D. (Eds.) Great White Sharks. The biology of *Carcharodon carcharias*: Chapter 9: Pp. 81-89.

Nambiar P, Bridges TE, Brown KA. (1991). Allometric relationships of the dentition of the great White Shark, *Carcharodon carcharias*, in forensic investigations of shark attacks. The Journal of forensic odonto-stomatology 9 (1): Pp. 1-16.

Natanson LJ & Skomal GB. (2015). Age and growth of the white shark, *Carcharodon carcharias*, in the western North Atlantic Ocean. Marine and Freshwater Research, Volume 66 (5): Pp. 387-398

Neil WH, Chang RKC, Dizon AE. (1976). Magnitude and ecological implications of thermal inertia in skipjack tuna, *Katsuwonus pelamis* (Linnaeus). Environmental Biology of Fishes, Volume 1, Issue 1, Pp. 61-80.

Noren DP. (2011). Estimated field metabolic rates and prey requirements of resident killer whales. Marine Mammal Science, 27(1): Pp. 60–77.

Osborne RW. (1999). A historical ecology of Salish Sea "resident" killer whales (*Orcinus orca*), with implications for management. Ph.D. Thesis, University of Victoria, Victoria, British Columbia.

Palomares MLD. & Pauly D. (1998). Predicting food consumption of fish populations as functions of mortality, food type, morphometrics, temperature and salinity. Marine and Freshwater Research, Volume 49, Issue 5, Pp. Pp. 447 – 453.

Pauly D, Trites AW, Capuli E, Christensen V. (1998). Diet composition and trophic levels of marine mammals. ICES Journal of Marine Science, 55: Pp. 467–481.

Pélabon C, Bolstad GH, Egset CK, Cheverud JM, Pavlicev M, Rosenqvist G. (2013). On the Relationship between Ontogenetic and Static Allometry. The American Naturalist; 181(2), Pp. 195-212.

Postel, E. (1958). Sur le presence de *Carcharodon carcharias* (L. 1758) dans les eaux tunisiennes. Bulletin du Muséum National d'Histoire Naturelle. Paris. (Ser. 2) 30: Pp. 342–244.

Robbins RL. (2007). Environmental variables affecting the sexual segregation of great white sharks *Carcharodon carcharias* at the Neptune Islands South Australia. Journal of Fish Biology, 70, Pp. 1350–1364.

Rohr JJ, Fish EF, Gilpatrick JW (2002). Maximum swim speeds of captive and free-ranging delphinids: critical analysis of extraordinary performance. Marine Mammal Science, 18(1): Pp. 1-19.

Sambilay, VC. (1990). Interrelationships between swimming speed, caudal fin aspect ratio and body length of fishes. Fishbyte, 8: 16-20.

Schmidt-Nielsen K. (1984). Scaling Why is Animal Size so Important? Cambridge University Press. ISBN: 9780521319874. Pp. 256.

Schmidt-Nielsen K. (1997). Animal Physiology: Adaptation and Environment. 5th Edition. Cambridge University Press. ISBN: 9780521570985. Pp. 617.

Schmidt-Nielson, K. (1972). Locomotion: energy cost of swimming, flying, and running. Science, New Series, Vol. 177, No. 4045, Pp. 222-228

Schwarz LK, Villegas-Amtmann S, Beltran RS, Costa DP, Goetsch C, Hückstädt L, Maresh JL, Peterson SH (2015). Comparisons and Uncertainty in Fat and Adipose Tissue Estimation Techniques: The Northern Elephant Seal as a Case Study. PLoS ONE 10(6): e0131877. doi:10.1371/journal.pone.0131877.

Secor SM. (2008). Specific dynamic action: a review of the postprandial metabolic response. Journal of Comparative Physiology B. Vol. 179(1): Pp.1–56.

Semmens JM, Payne NL, Huveneers C, Sims DW, Bruce BD. (2013). Feeding requirements of white sharks may be higher than originally thought. Scientific Reports 3, Article number: 1471: Pp. 1-4.

Semone SG & Syme DA. (2016). Elasmobranch Muscle Structure and Mechanical Properties. In: Brauner C.J., Farrell A.P., Shadwick, R.E. (Eds.). Physiology of Elasmobranch Fishes: Structure and Interaction with Environment. 1st Edition. ISBN: 9780128012895. Pp. 190-214.

Sepulveda CA, Kohin S, Chan C, Vetter R, Graham JB. (2004). Movement patterns, depth preferences, and stomach temperatures of free-swimming juvenile mako sharks, *Isurus oxyrinchus*, in the Southern California Bight. Marine Biology,

145 (1): Pp. 191-199. DOI: 10.1007/s00227-004-1356-0.

Sfakiotakis M, Lane DM, Davies JBC. (1999). Review of fish swimming modes for aquatic locomotion. IEEE Journal of oceanic engineering. Volume 24. Number 2. Pp. 237-252.

Sharp GD. & Vlymen WJ. (1978). II: The relation between heat generation, conservation, and the swimming energetics of tunas. In: Sharp GD & Dizon AE. (Eds.). The Physiological Ecology of Tunas. Proceedings of the Tuna Physiology Workshop hled at the National Marine Fisheries Service Southwest Fisheries Center La Jolla, California. Academic Press. Pp. 213-232.

Smale MJ & Cliff G. (2012). White shark and cephalopod prey. Indicators of habitat use? In: Domeier ML. (Ed.) Global Perspectives on the Biology and Life History of the Great White Shark. CRC Press: Chapter 4: Pp. 51-57.

Smit AJ, Roberts M, Anderson RJ, Dufois F, Dudley SFJ, Borman TG, Olbers J, Bolton JJ. (2013). A Coastal Seawater Temperature Dataset for Biogeographical Studies: Large Biases between In Situ and Remotely-Sensed Data Sets around the Coast of South Africa. PLoS ONE 8(12): e81944.

Spitz J, Mourocq E, Schoen V, Ridoux V. (2010). Short Communication: Proximate composition and energy content of forage species from the Bay of Biscay: high- or low-quality food? International Council for the Exploration of the Sea. Published by Oxford Journals. Pp. 909-915.

Stränger A.M. & Stobier W. (2001). Muscle fiber diversity and plasticity. In: Johnson I.A. (Eds.). Muscle Development and Growth, Fish Physiology. Volume 18: Pp. 187-250.

Syme DA & Shadwick RE. (2011). Red muscle function in stiff-bodied swimmers: there and almost back again. Philosophical Transactions of the Royal Society of London, Series B, Biological Sciences, 366 (1570): Pp. 1507-1515. DOI: 10.1098/rstb.2010.0322.

Tricas TC. & McCosker JE. (1984). Predatory behavior of the white shark (*Carcharodon carcharias*), with notes on its biology. Proceedings of the California Academy of Sciences. 43: Pp. 221–238.

Wardle CS. (1975). Limit of swimming speed. Nature, Volume 255. Pp. 725-727.

Webb PW. (1975). Hydrodynamics and energetics of fish propulsion. Bulletin of the Fisheries Research Board of Canada. Bulletin 190. Pp. 1-156.

Weltz K, Kock AA, Winker H, Attwood C, Sikweyiya M. (2013). The Influence of Environmental Variables on the Presence of White Sharks, *Carcharodon carcharias* at Two Popular Cape Town Bathing Beaches: A Generalized Additive Mixed Model. PLoS ONE 8(7): e68554. doi:10.1371/journal.pone.0068554.

Weng KC, Boustany AM, Pyle P, Anderson SD, Brown A, Block BA. (2007). Migration and habitat of white sharks (*Carcharodon carcharias*) in the eastern Pacific Ocean. Marine Biology 152: Pp. 877–894.

Williams TM. (1999). The Evolution of Cost Efficient Swimming in Marine Mammals: Limits to Energetic Optimization. Philosophical Transactions: Biological Sciences, Vol. 354, No. 1380. Pp. 193-201.

Winter SP & Cliff G (1999). Age and growth determination of the white shark, *Carcharodon carcharias*, from the east coast of South Africa. Fishery Bulletin, 97(1): Pp. 153-169.

Wolf N, Swift PR, Carey FG (1988). Swimming muscle helps warm the brain of lamnid sharks. Journal of Comparative Physiology B. Volume 157, Issue 6. Pp 709-715

Worthington LV. (1954). Three Detailed Cross-Sections of the Gulf Stream. Tellus, Volume 6, Issue 2, Pp. 116-123.

7. APPENDIX

Table A1: Measurements from specimens dissected for this study and their life history stage (*n* = 18).

Specimen	PCL (m)	FL (cm)	TL (m)	BM (kg)	MRMA (cm^2)	TRMM (kg)	RM$_\%$	CFH (mm)	Sex	Life History Stage
RB11025	1.21	133	1.52	25	6	0.5	2.0	N/A	F	Neonate
SUN09003	1.47	164	1.81	61	13.8	1.4	2.3	496	F	Neonate
TRA15004	1.58	179.8	1.96	67	19.40	2.2	3.3	540	M	Neonate
BAL11029	1.60	176	1.99	60	16.1	1.8	3.0	536	F	Neonate
UMT11011	1.64	184	1.99	77	14.7	1.7	2.2	572	M	Neonate
RB09037	1.83	211.6	2.30	88	18	2.4	2.7	560	M	Neonate
RB09033	1.93	215	2.31	120	18	2.4	2.0	560	M	Juvenile
RB09045	2.06	232	2.47	147	26.3	3.9	2.6	588	M	Juvenile
UMZ15002	2.09	232	2.52	154	38.1	5.6	3.6	700	M	Juvenile
UMH15006	2.10	236.2	2.52	150	41.8	6.2	4.2	740	F	Juvenile
RB15023	2.10	234	2.55	126	34.8	5.1	4.1	650	F	Juvenile
RB10034	2.16	240	2.67	154	24.9	3.8	2.5	630	F	Juvenile
RB15017	2.16	241	2.63	156	37.1	5.6	3.6	680	M	Juvenile
ZIN10030	2.31	259.8	2.82	260	31.5	5.2	2.0	804	F	Sub-adult
MG15028	2.31	254.2	2.71	188	40.7	6.5	3.5	668	F	Juvenile
ANS09017	2.49	279	3.04	222	27.1	4.8	2.1	860	F	Sub-adult
ANS10008	2.57	290	3.20	350	39.9	7.3	2.1	846	M	Sub-adult
ZIN09016	3.63	405	4.37	900	76.9	19.6	2.2	1320	F	Adult

Abbreviations: PCL = precuadal length, FL = fork length, TL = total length, BM = body mass, MRMA = mean red muscle area, TRMM = trunk red muscle mass, RM$_\%$ = red muscle percentage of body mass, CFH = caudal fin height.

Table A2: Modulated swimming speeds in the great white shark in km/h.

Life History Stage	Sustained swimming speed (km/h)		Burst swimming speed (km/h)		*n*
	Mean	Max	Mean	Max	
Neonate	5.7	6.2	33.2	35.9	65
Juvenile	6.8	7.7	39.4	44.4	189
Sub-adult	7.9	8.3	46.2	48.3	50
Adult	9.3	10.1	53.7	58.6	10